Journal of Stored Products Research xxx (xxxx) 102834

Contents lists available at ScienceDirect

Journal of Stored Products Research

journal homepage: www.elsevier.com/locate/jspr

Unraveling the properties of essential oil *of Mentha rotundifolia* (L.) Huds: Antimicrobial and antioxidant activities, and molecular docking

Meryem Benyamane [a], Iman Msegued Ayam [b], Soukaina Elorchi [c], Nouhaila Belasla [a], Imane Brahimi [a], Mohammed Salah [c], Faouzi Errachidi [b], Fatih Ozogul [d, e], Chakib El Adlouni [a], Abdellah Zinedine [a, *]

[a] *BIOMARE Laboratory, Faculty of Sciences, Chouaib Doukkali University, P.O. Box 20, El Jadida, 24000, Morocco*
[b] *Applied Organic Chemistry Laboratory, Faculty of Sciences and Technologies, Sidi Mohamed Ben Abdellah University, Route d'Imouzzer, Fez, Morocco*
[c] *Molecular Modeling and Spectroscopy Research Team, Department of Chemistry, Chouaïb Doukkali University, P.O. Box 20, El Jadida, 24000, Morocco*
[d] *Department of Seafood Processing Technology, Faculty of Fisheries, Cukurova University, Balcalı, Adana, 01330, Türkiye*
[e] *Biotechnology Research and Application Centre, Cukurova University, Balcalı, Adana, 01330, Türkiye*

ARTICLE INFO

Keywords:
Mentha rotundifolia
Essential oil
Antimicrobial
Antioxidant
Chemical composition
Molecular docking

ABSTRACT

This study aimed at investigating the biological activities (antibacterial, antifungal, and antioxidant), and the chemical profile of essential oil (EO) of *Mentha rotundifolia* planted in two Moroccan areas (*Marrakech* and *Taounate*). EO was extracted from plant leaves by Hydrodistillation and its chemical composition was determined using gas chromatography coupled with mass spectrometry (GC-MS/MS). The antimicrobial activity of extracted EO was tested against numerous microbial strains including bacteria, yeasts, and molds. While the antioxidant activity was assessed by four methods including β-carotene bleaching assay, free radical scavenging activity (DPPH), Ferric reducing antioxidant power (FRAP), and total antioxidant capacity (TAC). Results showed that rotundifolone ($C_{10}H_{14}O_2$) was the major component found in the EO of the plant collected from both studied areas, with 30.12 and 24.51 % in the EO of *Marrakech* and *Taounate,* respectively. Furthermore, 27 compounds were identified in the EO of *Marrakech,* including chlorcarvacrol (15.75 %) and piperitenone (6,09 %). While in the EO of *Taounate,* only 15 compounds were found including pulegone (19.11 %), and piperitenone (9.23 %). Significant antioxidant activity using the four tests was observed for EO of *Marrakech* compared to that of *Taounate*. Moreover, EO of *Marrakech* has a bactericidal effect, unlike a fungicidal effect observed with the EO of *Taounate.* These properties could be associated with the identified bioactive compounds in each study area. Molecular docking showed that the ligands synthesized have significant inhibitory potential against the tested strains and possesses strong antibacterial and antifungal activities, making them versatile candidates for developing broad-spectrum antimicrobial agents, and suggest the promising use of essential oil of *M. rotundifolia* as a natural preservative against a wide range of bacterial and fungal pathogens

1. Introduction

Essential oil (EO) are natural, volatile compounds extracted from various parts of aromatic and medicinal plants, widely recognized for their diverse biological properties and applications in the pharmaceutical, cosmetic, and food industries as natural flavorings and preservatives (Meenu et al., 2023; Puvača et al., 2021; Noshad et al., 2022). They have been particularly associated with their antimicrobial, antioxidant, and anti-inflammatory activities due to their complex mixtures of bioactive compounds, with phenolic monoterpenoids, making them valuable resources in both traditional and modern medicine (Khwaza and Aderibigbe, 2025).

One of the most crucial EO of aromatic and medicinal plants is that extracted from the leaves of *Mentha* species, stands up as a rather promising source of natural compounds exploited in the culinary and pharmaceutical sectors (Tafrihi et al., 2021). Thus, the active ingredients of EO of *Mentha* species mainly include terpenes, aldehydes, alcohols, ketones, alkaloids and other compounds (Li et al., 2025). On the other hand, around twenty species of this genus, including *M. piperita, M. pulegium, M. spicata,* and *M. rotundifolia*, etc., are nowadays ex-

* Corresponding author.
E-mail address: zinedine.a@ucd.ac.ma (A. Zinedine).

https://doi.org/10.1016/j.jspr.2025.102834
Received 31 July 2025; Received in revised form 25 September 2025; Accepted 25 September 2025
0022-474/

ploited for their medicinal properties, most notably for the preparation of many conventional therapeutic infusions (El Hassani, 2020).

Morocco a North African and Mediterranean country, with nearly 3400 km of coastline and a geographical position ranging from seas to deserts and mountains, benefits from a variety of climatic zones favoring the abundance of a wide variety of wild plants, thus offering an exceptional environment for the cultivation of aromatic and medicinal plants (El Hassani, 2020). Indeed, some *Mentha* species have been extensively investigated in the country, by way of example the EO of *M. pulegium* in *Taounate* region brings a significant income, reaching 6.12 million MAD a year (0.6 million US$). Moreover, according to the Ministry of Agriculture and Marine Fisheries, *M. spicata*, which grows on 3000 ha, generates about 85,000 tons, most of which are exported. Commonly employed in traditional healthcare to treat digestive and respiratory diseases, *Mentha* species are highly valued for their biological properties including antibacterial, antifungal, and antioxidant activities (Yousefian et al., 2023).

Nevertheless, other *Mentha* species remain understudied despite their potential value and the increasing demand for novel natural bioactive compounds (Riaz et al., 2021). In this context *Mentha rotundifolia* locally known as *"Timarssate", "Marssita", "Mchichtrou"* or *"Timijja"* emerges a promising candidate for valorization, which is traditionally used for therapeutic purposes in treating digestive problems, tooth discomfort, skin infections, and as a tonic or sedative (Brahmi et al., 2015; Ladjel et al., 2011), and it is a culinary plant that flavors many drinks, such us Moroccan mint tea. Even though *M. rotundifolia* is a well-known medicinal and aromatic plant in the country and traditionally used in different sectors, and despite its recognized properties, its EO is still underexplored, providing an opportunity to investigate its properties and its possible use in future food and healthcare applications. Furthermore, no studies are yet available on the effect of climatic factors that may affect the EO chemical profile and its biological activities.

In light of these considerations, the present study aimed at assessing the biological properties (antibacterial, antifungal, and antioxidant) of EO extracted from *M. rotundifolia* leaves planted in two Moroccan areas (*Marrakech* and *Taounate*), at identifying the EO chemical components using gas chromatography and tandem mass spectrometry (GC-MS/MS), and lastly at performing a molecular docking analysis to highlight the binding affinities between the main EO bioactive components and microbial receptor targets used in this study.

2. Material and methods

2.1. Sampling of M. rotundifolia

Leaves of *M. rotundifolia* were collected in May 2023 from two sites, *Taounate* and *Marrakech* (Fig. 1). The geographical coordinates of *Taounate* sampling site are as follows: Latitude: (34° 32′ 09″), longitude (4° 38′ 24″), and altitude (566 m). *Taounate* is a mountainous area located in northern Morocco having a semi-humid climate with a strong continental influence, and an average annual temperature of 17–18 °C and precipitations of 650–700 mm. The soil is dominated by clayey or loamy textures with high levels of limestone ($CaCO_3$) and exchangeable calcium, and neutral to slightly alkaline pHs. Regarding *Marrakech* sampling site (latitude: 31° 37′ 46″, longitude: 7° 58′ 52″, and altitude: 457 m), the climate is arid with average annual temperature of 21 °C and precipitations of 250–300 mm. While the soil consists of poorly evolved soils in the mountain areas and alluvium along the rivers, with a predominance of diverse parent rocks such as sandstones, clays and marls, as well as outcrops of primary and tertiary rocks in the High Atlas.

The identity of the studied plant was confirmed by Dr. Chaimae Rais, Botanist at ANPMA (National Agency of Aromatic and Medicinal Plants), based on morphological comparison with monographs and verification against authentic samples from recognized botanical gardens of ANPMA (Morocco).

Plant material were dried in the shade at room temperature for about two weeks and followed by grinding since this technique remains the most effective technique for preserving and maximizing essential oil yield in Lamiaceae family, as recently reported (Hazrati et al., 2021; Rana et al., 2021; Yeddes et al., 2022).

2.2. Essential oil extraction

Essential oil was extracted from *M. rotundifolia* leaves using Clevenger-type apparatus (Jeulin, Paris, France), a technique widely used for extracting EO while preserving its chemical properties. For this, 100 g of leaves powder were distilled in distilled water (1 L) during 3h. The recovered EO was stored in a brown vial at 4C°, preserving its quality until further analysis (Wahba et al., 2020). The EO yield was calculated according to equation n° 1, as follows (Thakker et al., 2016):

$$Yield\ (\%) = \frac{\text{EO weight (g)}}{\text{Weight of the dried plant material (g)}} \times 100 \qquad \text{(Equation n°1)}$$

2.3. GC-MS/MS analysis

A gas chromatography-mass spectrometer (GC-MS triple Quadrupole TQ) system (SHIMADZU Corporation, GCMS TQ 8040NX, Vogelsang, USA) was used to determine the chemical composition of the extracted EO. This technique is considered the gold standard for the identification and quantification of volatile compounds in EO (Chauhan, 2014).

EO analysis was performed using a DB1 fused silica capillary column (30m × 0.25 mm ID x 0.25 μm; Restek, Bellefonte, USA) under identical temperature conditions. Sample injection was carried out with a split ratio 1:200. Mass spectral data were obtained using the REAL time software (Shimadzu corporation, Vogelsang, USA), and the chemical components were identified by comparison with the NIST library (version 2019). Spectral scanning was conducted within the 35–500 m/z (mass-to-charge) range, and the relative percentages of the chemical components were determined by calculating the peak areas.

2.4. Antioxidant activity

2.4.1. DPPH test

The free radical scavenging activity (DPPH) of the extracted EO was assessed by a method recently reported by Jeldi et al. (2022). In this assay, 2 mL of 60 μM DPPH solution were added to 500 μL of each EO, previously prepared at a concentration of 5 mg/mL in ethanol. After incubation for 30 min away from light at room temperature, the absorbance was measured at 517 nm. The scavenging activity (%) was calculated using equation (2), as follows:

$$\text{Radical scavenging percentage } (\%) = \frac{\text{DPPH Abs} - \text{EO sample Abs}}{\text{DPPH AbS}} \times 100 \text{(Eq}$$

Where,

- DPPH Abs: Absorbance of the control solution measured at 517 nm,
- EO sample Abs: Absorbance of the EO sample measured at 517 nm.

2.4.2. β-carotene bleaching assay

The β-carotene bleaching assay used in this study was the protocol reported by Miraliakbari and Shahidi (2008) and slightly modified. In a tube containing 1 mL of chloroform, β-carotene (0.5 mg) was dissolved. Thereafter, 25 μL of linoleic acid and 200 mg of tween 80 were added. The chloroform was then evaporated at 45 °C, and 100 mL of oxygen-

saturated distilled water were added to the mixture under vigorous stirring to form an emulsion. Subsequently, 2 ml of the β-carotene emulsion were mixed with 500 μL of EO previously prepared at a concentration of 5 mg/mL in ethanol. The absorbance of the mixture was measured at 470 nm, both at time zero and after incubation for 2h in a water bath at 50 °C (Reis et al., 2012). The antioxidant activity (%) was calculated using equation (3), as follows (Carneiro et al., 2013):

$$\text{Antioxidant activity (\%)} = \frac{\text{Absorbance after t (min)}}{\text{Initial absorbance}} \times 100 \quad \text{(Equation n°3)}$$

2.4.3. Total antioxidant capacity test

The total antioxidant capacity (TAC) was evaluated according to the method of Maškovič et al. (2012) with slight adjustments. Thus, 200 μL of each EO sample were combined with 2 mL of the reagent (0.6 M sulfuric acid, 28 mM sodium phosphate, and 4 mM ammonium molybdate). After incubation for 90 min at 95 °C, the absorbance was measured at 695 nm using an UV-5100 spectrophotometer (Shanghai Metash Instruments Co., Ltd., Shanghai, China). The TAC value was reported as milligrams of ascorbic acid equivalent per gram of EO (mg EAA/g EO) by reference to a standard curve of ascorbic acid.

2.4.4. Ferric reducing antioxidant power test (FRAP)

This assay was performed in accordance with the method reported by Moattar et al. (2016). Briefly, 500 μL of phosphate buffer (0.2 M; pH = 6.6) and 500 μL of potassium ferricyanide [$K_3Fe(CN)_6$] (1 %) were incorporated into 100 μL of each EO in different concentrations prepared in ethanol. After incubation for 20 min at 50 °C in a thermostatic heater water bath Cu-600 (West Tune, China), 500 μL of TCA (10 %), 100 μl FeCl3(0.1 %) and 500 μl of distilled water were subsequently added to the reaction medium. Absorbance readings were taken at 700 nm. The results are presented in effective concentration at 50 % (EC-50), which indicates the antioxidant concentration needed to acquire an absorbance of 0.5 nm.

2.5. Antimicrobial activity

The antimicrobial activity of extracted EO was evaluated against a variety of microbial species, including 8 Gram-positive and Gram-negative bacteria supplied by the Institut Pasteur (Casablanca). The Gram + bacteria included *Bacillus cereus* ATCC 33019, *Bacillus subtilis* ATCC 6633, *Enterococcus faecalis* CIP 103214, *Staphylococcus aureus* ATCC 9144, and *Streptococcus agalactiae* IPM 24842, while the Gram- bacteria were *Escherichia coli* CIP 54127, *Providencia alcalifaciens* CIP 82.90T, and *Salmonella typhi* CIP 5535. Finally, the 2 tested mold strains (*Aspergillus flavus* ATCC 1015 and *Aspergillus niger* NRRL 3357) and the 3 yeast strains (*Candida tropicalis*, *Rhodotorula* spp., and *Saccharomyces cerevisiae)* are part of the BIOMARE laboratory's (UCD-El Jadida) microbial collection.

2.5.1. Disk agar diffusion

This method was used to assess the antibacterial activity of the EO. For this, sterile paper discs (Ø, 6 mm), each impregnated with 10 μL of EO, were placed on Mueller-Hinton agar (Biokar Diagnostics, France) plates that had been inoculated with bacterial suspensions at 10^7–10^8 CFU/mL (optical density 0.08–0.1 at 625 nm, based on the McFarland scale). The plates were incubated for 24 h at 37 °C, and the diameter of inhibition zones (mm) were measured to determine the antibacterial activity.

2.5.2. Agar well diffusion assay

This assay was performed to assess the EO activity against yeast strains. Briefly, wells of 6 mm diameter were perforated in plates containing yeast extract peptone glucose agar. Then, 25 μL of an EO solution (composed of 10 μL pure oil and 15 μL DMSO at 5 %) were added to each well. For positive control, 25 μL of amphotericin B (Amp B) at 100 μg/mL were used. Yeast suspensions were prepared in 0.9 % NaCl, with an optical density of 0.04 at 630 nm, corresponding to 10^7 spores/mL. Diameters of inhibition zones were measured after incubating the plates at 30 °C for 48–72 h.

2.5.3. Agar incorporation method

To evaluate the EO activity against mold strains, 50 μL of pure EO were mixed with 450 μL of 0.2 % molten agar and combined with 19.5 mL of potato dextrose agar (Biokar Diagnostics, France). Similarly, for the positive control, 100 μg of Amp B were dissolved in 450 μL of 0.2 % agar, mixed with 19.5 mL of PDA, and used to prepare the control plates. Following gelation, a piece of mold strains was positioned in the middle of the (90 mm) petri dishes that had been filled with the various formulations and then incubated at 27 °C for 72–96h.

2.5.4. Determination of MIC, MBC and MFC

The minimum fungicidal concentration (MFC) and the minimum bactericidal concentration (MBC) are the concentrations needed to kill microorganisms, whereas the minimum inhibitory concentration (MIC) is the lowest concentration needed to prevent microbial growth. The broth dilution technique was used to determine MBC, MFC and MIC values of each tested EO (Cosentino et al., 1999). The antibacterial activity of EO was measured in the nutrient broth (Biokar Diagnostics, France) and incubated for 24h at 37 °C. While the antifungal activity of the EO was assessed in the yeast peptone glucose broth (Biokar Diagnostics, France). Molds and yeasts were incubated for 72h at 27 °C and 48h at 30 °C, respectively.

2.6. Molecular docking

The molecular geometry was optimized using Gausian 09 (Frisch et al., 2009) to ensure accurate ligand structures and their electronic proprieties. Density Functional Theory (DFT) calculations were conducted with B3LYP level of theory (Lecklider, 2011) and the 6-31G + (d,P) basis set. Initial 3D structures of ligands and receptors were obtained from the PDB (protein data bank) and pre-processed by removing water molecules and ions. This step ensured that the ligands adopted their lowest energy conformations, which is essential for reliable docking simulations. To predict binding orientations and affinities, AutoDock Vina (Trott and Olson, 2010) was used to carry out molecular docking simulations. The docked complexes were further refined using Gaussian 09 for structural and electronic optimization. Docking results visualization and analysis were conducted using the software BIOVIA Discovery Studio 2025, which facilitated the examination of molecular interactions and identification of potential binding sites. This approach ensured accurate modeling of ligand-receptor interactions for subsequent analysis.

2.7. Statistical analysis

All analyses used in this study were carried out in triplicate. Student (T-test) and variance analysis (ANOVA) test were conducted to compare the means of obtained results, which are given as ± standard deviation (SD).

3. Results and discussion

3.1. Essential oil yield

The yield of EO (%) from the two study areas are nearly identical, with values of 0.33 % for *M. rotundifolia* of *Marrakech* (MRM) and 0.30 % for *M. rotundifolia* of *Taounate* (MRT), respectively.

The EO yield showed minor variation, even though the sites differ in climate and soil composition. This observation indicates that under the conditions of the present study, environmental variables may play a minor role in determining EO yield for *M. rotundifolia*. These findings

aligned with previous studies in which modifications in soil properties or amendments did not lead to statistically significant differences in essential oil yield. For example, Mwithiga et al. (2022) reported that rosemary plants exhibited similar EO yields across various soil amendment treatments, while Gathara et al. (2022) observed no significant variation in oil yield among sandalwood trees from multiple sites despite differences in soil nutrient content.

The EO yields obtained in the present study are relatively low in comparison with previous studies conducted on other *Mentha* species, but similar to those observed in some aromatic and medicinal plants known for their relatively low oil content. For example, a recent study from India has reported low yields of EO extracted from many *Mentha* species, including *M. arvensis, M. piperita* and *M. spicata*, with respectively 0.5, 0.9 and 0.8 % (Tewari et al., 2024). Regarding EO of *M. rotundifolia*, a previous study of Derwich et al. (2010) reported a yield of 1.54 %, indicating that yields from other *Mentha* species have been higher, such as the Moroccan *M. puleguim*, with yield of 1.66 %. On the other hand, EO extracted from the Chinese *M. haplocalyx*, showed yields ranging from 0.5 to 3 % (Zhao et al., 2013). Controversially, a recent study conducted in Morocco, reported a high EO yield of 1.58 % for *M. rotundifolia* (Sbai et al., 2023). On the other hand, the yield of EO extracted from *Myrtus communis* was reported to be 0.30 % (Aidi Wannes et al., 2010). These low yields are similar to those obtained when the essential oil was extracted from *Pinus brutia* with a yield of around 0.40 %, while the EO extracted from *Pinus sylvestris* had a much lower yield of around 0.13 % (Tumen et al., 2010).

It has been reported that several factors, both internal and external, could have a direct influence and therefore may impact on the variability of EO yields, such as climatic and environmental conditions, studied species, variety, harvest period, maturity stage, leaf drying technique, senescence of harvested leaves, and finally the method used for EO extraction (Calo et al., 2015).

3.2. Determination of EO components

The GC-MS/MS chromatograms of the EO analysis are illustrated in Fig. S1. As shown, the chemical components of the extracted EO from leaves of MRM and MRT reveal different profiles between the two sampling areas. Indeed, each chromatogram displays peaks corresponding to distinct compounds, reflecting the complexity and diversity of the EO composition. The comparison of the two chromatograms highlights regional variations that may be attributed to specific environmental conditions. The identified compounds, their relative percentages, retention indices (RI), and retention times (RT) are presented in Table 1.

As shown, rotundifolone was the most abundant compound found in both EO, with 30.12 % in MRM and 24.51 % in MRT. EO extracted from MRM was more complex, containing 27 compounds that made up 96.26 % of the total composition. The second major compound found in MRM was chlorcarvacrol (15.75 %). Other significant compounds included piperitenone (6.09 %) and pulegone (4.47 %).

On the other hand, EO extracted from MRT contained only 15 compounds, representing 97.57 % of total EO composition. The major component found was rotundifolone (24.51 %), followed by pulegone (19.11 %), piperitenone (9.23 %), and tetrapentacontane isomers (11.14 %). Few amounts of p-Menth-3-en-8-ol (6.24 %) and caryophyllene (4.78 %) were also present.

Both EO extracted from MRT and MRT shared several minor compounds, such as terpinen-4-ol and germacrene D, with variations in their concentrations. Additionally, each EO had unique compounds that may highlight the influence of regional factors on the chemical profile of EO of *M. rotundifolia*. Based on the GC-MS/MS analysis, this study is the first to identify rotundifolone as the major component of the EO extracted from the leaves of *M. rotundifolia* in Morocco. In fact, no previous study conducted in the country has listed the presence of this component as a significant constituent of EO of *M. rotundifolia* planted in different areas, which underlines the novelty of the obtained results in the present study.

Similarly, this compound has previously been reported in neighboring countries as the major compound of the EO of this plant. Indeed, Aouadi et al. (2021) identified rotundifolone as the dominant component (46.06 %) in the EO of Algerian *M. rotundifolia*. While in another Algerian study, Yakhlef et al. (2020) reported caryophyllene oxide (35.27 %) and piperitenone oxide (35.49 %) as the major components of the EO, illustrating notable regional variations. Moreover, rotundifolone and other chemical compounds have been identified as the primary ingredients of EO in Tunisia (Ben Haj Yahia et al., 2019), with variations based on ecological and climate conditions. Compared with other species of the genus *Mentha*. El Omari et al. (2024) has recently reported that compulegone (17.56 %), mintlactone (10.62 %) and D-carvone (9.24 %) predominate in the EO of *M. piperita*. Similarly, Sah et al. (2024), reported the dominance of piperitenone oxide (31.3 %) and cis-piperitone oxide (51.61 %) in the EO of *M. longifolia*. Furthermore, high percentages of menthol (71.31 %) and menthone (13.34 %) were reported in the EO of *Mentha arvensis* (Alonso Leite dos Santos et al., 2024), that are insignificant for *M. rotundifolia*.

3.3. Antioxidant activity

Table 2 summarizes the antioxidant activity using four complementary methods (β-carotene bleaching assay, DPPH, FRAP, and TAC). These assays provided a comprehensive overview of *M. rotundifolia* EO ability to neutralize free radicals and reduce oxidative stress.

According to the DPPH method, MRM exhibits high antioxidant activity with an IC_{50} of 0.03 ± 0.02 mg/mL, as compared to that of MRT (IC_{50} of 0.05 ± 0.07 mg/mL). The results obtained from the other three methods (β-carotene bleaching assay, FRAP, and TAC) corroborated the results of the first assay (DPPH), demonstrating that EO of MRM has higher antioxidant activity (IC_{50} of 0.7 ± 0.01 mg/mL), (EC_{50} 0.03 ± 0.01 μg/mL) and (11.00 ± 0.05 mg EAA/g EO), when compared to those of MRT (IC_{50} of 1.6 ± 0.02 mg/mL), (EC_{50} 0.33 ± 0.02 μg/mL) and (10.07 ± 0.01 mg EAA/g EO).

These findings are similar to those of Riahi et al. (2013), who reported that EO of *M. rotundifolia* in two Tunisian localities has substantial antioxidant activity, particularly the EO of *M. rotundifolia* collected in *Beja* (IC_{50} = 0.03 mg/mL). Similarly, a comparable antioxidant activity (IC_{50} of 0.02 mg/mL) of EO of *M. rotundifolia* was reported from Iran (Nickavar et al., 2008). Results of FRAP method were consistent with those reported by Salamatullah (2022), who found an EC_{50} value of 0.35 ± 0.03 mg/mL for EO from *M. rotundifolia* leaves, indicating a comparable and considerable antioxidant activity. Beyond the previously assays, The EO exhibited a notably high TAC value of (11.00 ± 0.05 mg EAA/g EO) for MRM and (10.07 ± 0.01 mg EAA/g EO) for MRT, reflecting its strong capacity to neutralize oxidative agents. This results is comparable to (Chebbac et al., 2022), which showed a TAC value of 7.299 ± 1.774 mg EAA/g of the EO of *Artemisia aragonensis*.

It should be noted that several factors can impact the antioxidant activities of EO, including their chemical composition, the methodologies used for testing, as well as the EO extraction protocol used (Khodaei et al., 2021). According to Gulluce et al. (2007), the presence of phenolic compounds and other metabolites is principally responsible for the EO potential for significant antioxidant activity. The obtained results in the present study agree with previous finding of Benabdallah et al. (2016), who reported similar results in the radical-scavenging of EO from *Mentha* species highlighting the critical role of oxygenated monoterpenes in enhancing antioxidant activity. Additionally, compounds such as pulegone and menthol, also identified in the EO of *M. rotundifolia*, contribute to their antioxidative potential due to their known free radical-neutralizing properties.

Table 1
Chemical composition of EO of *M. rotundifolia* from *Marrakech* and *Taounate* analyzed by GC-MS/MS.

No	Compounds	Formula	RI	MW	RT	MRT (%)	MRM (%)
1	Menthomenthene	$C_{10}H_{16}$	1018	136	11.971	1.6	–
2	p-Menth-3-en-8-ol	$C_{10}H_{18}O$	1143	154	14.318	6.24	–
3	Terpinen-4-ol	$C_{10}H_{18}O$	1137	154	15.231	1.45	1.93
4	Endo-Borneol	$C_{10}H_{18}O$	1138	154	14.98	–	1.32
5	Pulegone	C10H16O	1212	152	16.873	19.11	4.47
6	cis-Piperitone epoxide	$C_{10}H_{16}O_2$	1171	168	17.291	–	3.64
7	Rotundifolone	$C_{10}H_{14}O_2$	1236	166	20.23	21.90	27.95
8	Iso-rotundifolone	$C_{10}H_{14}O_2$	1236	166	18.17	2.61	2.10
9	Piperitenone	$C_{10}H_{14}O$	1223	150	19.628	9.23	6.09
10	2-Undécanone	$C_{10}H_{18}O$	1251	170	18.35	–	0.48
11	Thymol	$C_{15}H_{32}$	1262	150	18.275	–	1.53
12	Carvacrol	$C_{10}H_{14}O$	1262	150	18.51	–	3.73
13	8.9-Déhydrothymol	$C_{10}H_{12}O$	1293	148	16.215	–	1.13
14	Farnesane	$C_{15}H_{32}$	1320	212	11.482	1.79	–
15	Farnesane	$C_{15}H_{32}$	1320	212	12.835	1.58	–
16	Dodecane, 2,6,11-trimethyl- +	$C_{15}H_{32}$	1320	212	17.896	2.47	–
17	Dodecane, 2,6,11-trimethyl-	$C_{15}H_{32}$	1320	212	19.167	2.5	–
18	cis-Jasmone	$C_{11}H_{16}O$	1338	164	21.037	–	0.78
19	γ-Cadinene	$C_{15}H_{24}$	1435	204	24.152	–	0.38
20	Bicyclosesquiphellandrene	$C_{15}H_{24}$	1435	204	22.9	–	1.02
21	Cinerolon	$C_{10}H_{14}O_2$	1426	166	21.176	–	4.73
22	Caryophyllene	$C_{15}H_{24}$	1494	204	21.852	4.78	3.24
23	Germacrene D	$C_{15}H_{24}$	1515	204	23.378	3.04	2.2
24	Eicosane isomers (C20H42)	$C_{20}H_{42}$	2009	282	25.78	7.08	–
25	Calamenen-10-ol	$C_{15}H_{22}$	1537	202	24.323	–	1.6
26	Spathulenol	$C_{15}H_{24}O$	1536	220	25.899	–	1.38
27	β-Caryophyllene epoxide	$C_{15}H_{24}O$	1507	220	26.082	–	2.78
28	Chlorcarvacrol	$C_{10}H_{13}ClO$	1505	184	25.523	–	15.75
29	Hydrocoumarin	$C_{10}H_{10}O_2$	1505	162	20.131	–	1.48
30	p-Mentane-1,2,3-triol	$C_{10}H_{20}O_3$	1503	188	21.416	–	2.38
31	δ-Cadinene	$C_{15}H_{24}$	1469	204	24.26	–	0.53
32	Hexadecane	$C_{16}H_{34}$	1612	226	21.249	1.05	–
33	τ-Muurolol	$C_{15}H_{26}O$	1580	222	28.144	–	1.21
34	Viridiflorol	$C_{15}H_{26}O$	1530	222	26.444	–	1.07
35	α-Humulene	$C_{15}H_{24}$	1579	204	22.745	–	0.48
36	6-Isopropenyl-4,8a-dimethyl-1,2,3,5,6,7,8,8a-octahydro naphtalen-2-ol	$C_{15}H_{24}O$	1690	220	29.097	–	0.81
37	Tetrapentacontane isomers	$C_{54}H_{11}0$	5389	758	35.6	11.14	–
Oxygenated monoterpenes						60.54	57.05
Sesquiterpene hydrocarbons						11.19	7.85
Non-terpenic						24.24	17.71
Oxygenated sesquiterpenes						–	13.58
Monoterpene hydrocarbons						1.6	
Total						97.57	96.19

***Note*:** MRM: *M. rotundifolia* from *Marrakech*; MRT: *M. rotundifolia* from *Taounate*. Compounds are arranged by retention indices (RI) and include molecular weight (MW), retention times (RT), and their relative percentages (%) in each analyzed EO.

Table 2
Antioxidant activity of EO of *M. rotundifolia* from *Marrakech* and *Taounate* based on DPPH and β-Carotene Bleaching assays (IC50 Values). *Note*. Values represent means ± SD (standard deviation) for triplicate experiments.

Antioxidant activity tests	*Study area*	
	Marrakech (MRM)	Taounate (MRT)
DPPH (IC_{50} mg/mL)	0.03 ± 0.02	0.05 ± 0.07
β-carotene bleaching (IC_{50} mg/mL)	0.7 ± 0.01	1.6 ± 0.02
FRAP (EC_{50} µg/mL)	0.03 ± 0.01	0.33 ± 0.02
TAC (mg EAA/g EO)	11.00 ± 0.05	10.07 ± 0.01

Note: The IC_{50} values of DPPH and β-carotene bleaching assays represent the effective concentration of EO (mg/mL) required to achieve 50 % antioxidant activity. The FRAP results are expressed as the concentration of EO (mg/mL) needed to reach an absorbance of 0.5 at 700 nm. TAC results are expressed in mg of ascorbic acid equivalent per gram of EO (mg EAA/g EO).

The prominence of rotundifolone in both regional samples underscore its importance as a key bioactive compound, setting the antioxidant profile of *M. rotundifolia* apart from other *Mentha* species where phenolic compounds or hydrocarbons may dominate. This highlights the unique chemotype of the EO from MRM and MRT, emphasizing their specific bioactive potential driven by their distinctive chemical composition.

3.4. Antimicrobial activity

The antibacterial and antifungal activities of EO of *M. rotundifolia* planted in *Marrakech* and *Taounate* were assessed using the disk diffusion method and MIC/MBC or MIC/MFC determination against both Gram + and Gram-bacteria, yeasts and fungal strains. Results of these activities are presented in Table 3.

3.4.1. Antibacterial activity

Regarding the antibacterial activity, significant inhibition zone diameters were obtained with the EO of MRM against *E. coli* CIP 54127 (16.16 ± 0.3 mm), *S. typhi* CIP 5535 (17.33 ± 0.3 mm), *B. subtilis* ATCC 6633 (18.66 ± 0.6 mm), and *E. faecalis* CIP 103214 (19.66 ± 0.3 mm). While the high inhibition zone diameters of the EO of MRT were reached against *B. subtilis* ATCC 6633 (15.6 ± 0.1 mm), *E. coli* CIP 54127 (15 ± 0.3 mm), and B. *cereus* ATCC 33019 (14 ± 0.05 mm). Results summarized in Table 3 demonstrates signifi-

Table 3
Antimicrobial activity of *M. rotundifolia* EO from *Marrakech* and *Taounate* areas. *Note*. *Note*. Values represent means ± SD (standard deviation) for triplicate experiments.

	MIC (µL/mL)			MBC or MFC (µL/mL)			MBC or MFC/MIC	Effect
Bacterial strains	***EO***		***Strep (µg/mL)***	***EO***		***Strep (µg/mL)***		
E. coli CIP 54127	MRM	1.46 ± 0.01	10 ± 0.01	MRM	22.86 ± 0.01	10 ± 0.01	15.65	Bacteriostatic
	MRT	9.14 ± 0.01		MRT	22.86 ± 0.01		2.50	Bactericidal
P. alcalifaciens CIP 82.90T	MRM	3.65 ± 0.01	30 ± 0.01	MRM	9.14 ± 0.01	90 ± 0.01	2.50	Bactericidal
	MRT	3.65 ± 0.01		MRT	9.14 ± 0.01		2.50	Bactericidal
S. agalactiae	MRM	3.65 ± 0.01	30 ± 0.01	MRM	9.14 ± 0.01	30 ± 0.01	2.50	Bactericidal
IPM 24842	MRT	3.65 ± 0.01		MRT	9.14 ± 0.01		2.50	Bactericidal
Salmonella typhi CIP 5535	MRM	3.65 ± 0.01	90 ± 0.01	MRM	3.65 ± 0.01	90 ± 0.01	1	Bactericidal
	MRT	3.65 ± 0.01		MRT	9.14 ± 0.01		2.50	Bactericidal
E. faecalis	MRM	3.65 ± 0.01	0.22 ± 0.01	MRM	9.14 ± 0.01	0.57 ± 0.01	2.50	Bactericidal
CIP 103214	MRT	9.14 ± 0.01		MRT	57.14 ± 0.01		6.25	Bacteriostatic
B. subtilis ATCC 6633	MRM	0.58 ± 0.01	0.13 ± 0.01	MRM	3.65 ± 0.01	0.32 ± 0.01	6.29	Bacteriostatic
	MRT	1.46 ± 0.01		MRT	22.86 ± 0.01		15.65	Bacteriostatic
S. aureus ATCC9144	MRM	1.46 ± 0.01	0.22 ± 0.01	MRM	3.65 ± 0.01	0.57 ± 0.01	2.50	Bactericidal
	MRT	9.14 ± 0.01		MRT	22.86 ± 0.01		2.50	Bactericidal
B. cereus	MRM	0.58 ± 0.01	30 ± 0.01	MRM	1.46 ± 0.01	90 ± 0.01	2.51	Bactericidal
ATCC 33019	MRT	3.65 ± 0.01		MRT	9.14 ± 0.01		2.50	Bactericidal
Fungal strains	***EO***		***Amp B (µg/mL)***	***EO***		***Amp B (µg/mL)***		
C. tropicalis	MRM	2.13 ± 0.01	01.06 ± 0.01	MRM	10.80 ± 0.01	01.06 ± 0.01	5.07	Fungistatic
	MRT	2.13 ± 0.01		MRT	2.13 ± 0.01		1	Fungicide
Rhodotorula spp.	MRM	2.13 ± 0.01	12.15 ± 0.01	MRM	10.80 ± 0.01	12.15 ± 0.01	5.07	Fungistatic
	MRT	0.42 ± 0.01		MRT	0.94 ± 0.01		2.23	Fungicide
S. cerevisiae	MRM	123.07 ± 0.01	R	MRM	R	R	–	Fungistatic
	MRT	123.07 ± 0.01		MRT			–	Fungistatic
A. niger	MRM	0.46 ± 0.01	27.07 ± 0.01	MRM	12.00 ± 0.01	R	26.08	Fungistatic
ATCC 1015	MRT	0.46 ± 0.01		MRT	01.05 ± 0.01		2.28	Fungicide
A. flavus	MRM	0.46 ± 0.01	0.47 ± 0.01	MRM	5.33 ± 0.01	0.47 ± 0.01	11.58	Fungistatic
NRRL 3357	MRT	0.46 ± 0.01		MRT	0.46 ± 0.01		1	Fungicide

Note: MRM: *M. rotundifolia* from *Marrakech*, MRT: *M. rotundifolia* from *Taounate*, MIC: minimum inhibitory concentration, MBC: minimum bactericide concentration, MFC: minimum fungal concentration. Values related to the EO are expressed in **µL/mL**, whereas those for the positive control:(Strep: streptomycin for antibacterial activity and Amp B: Amphotericin B for antifungal activity) are expressed in ***µg/ml***.

cant antibacterial efficacy of the EO of both MRM and MRT against all tested Gram + and Gram-bacteria.

As indicated, the EO of MRM showed higher antibacterial activity than the EO of MRT for most tested bacterial strains. This trend highlights the superior potency of EO of MRM against Gram + bacteria. In comparison, most of the tested strains were resistant to penicillin (positive control), underlining the potential of EO of *M. rotundifolia* as effective natural antibacterial agents.

Results of the MIC and MBC provide deeper insights into the bacteriostatic and bactericidal properties of the tested EO. As shown, EO of MRM and MRT had a bactericidal effect on *B. cereus* ATCC 33019, *P. alcalifaciens* CIP 82.90T, *S. agalactiae* IPM 24842, *S. typhi* CIP 5535, *S. aureus* ATCC9144 with MBC/MIC values ranging from 1 to 2.51. Moreover, both EO of MRM and MRT had a bacteriostatic effect on *B. subtilis* ATCC 6633 with MBC/MIC values of 6.29 and 15.65, respectively.

On the other hand, EO of MRM exhibited notably lower MIC values compared to those of the EO of MRT for most used bacterial strains, highlighting its higher antibacterial potential. For instance, The MIC and MBC of EO of MRM on *B. cereus* ATCC 33019 were 0.58 and 1.46 µL/mL, respectively. Conversely, MIC and MBC of EO of MRT were 3.65 and 9.14 µL/mL to achieve the same effects on the tested strain. This pattern is also valid for other strains such as *S. aureus* ATCC9144, where the MBC and MIC values for EO of MRM were 3.65 and 1.46 µL/mL, respectively. These findings perfectly agree with previous studies demonstrating the significant antibacterial potential of EO. of *M. rotundifolia*. Indeed, studies from Tunisia highlighted the EO strong efficacy, particularly against *E. coli* (Riahi et al., 2013). Similarly, a considered antibacterial effect of EO of *M. rotundifolia* was reported against several pathogenic bacteria, including *S. aureus* and *Listeria monocytogenes*, exhibiting inhibition zones of 22.33 ± 2.08 and 29.33 ± 0.57 mm, respectively (Yakoubi et al., 2024).

Compared to other *Mentha* species, the EO of *M. rotundifolia* showed comparable or even superior antibacterial potential. Indeed, Messaoudi et al. (2022) found an inhibition zone diameter of 37.33 mm against *S. aureus* using EO *of M. pulegium*, while Saba et al. (2024) reported a high antibacterial activity (39 mm) of *M. spicata* EO from Pakistan against *B. subtilis*. Furthermore, Talbaoui (2012) reported that the MIC/MBC values of EO of Moroccan *M. viridis* and *M. piperita* against *E. coli* were 2.5/2.5 and 10/10 µL/mL, respectively. In comparison, findings of the present work revealed a strong antibacterial activity of EO of MRM, which exhibited a MIC of 1.46 µL/mL against *E. coli*, indicating higher efficacy than the aforementioned species.

As reported in previous studies, the antibacterial activity of EO is essentially due to its capability to interfere with critical bacterial processes (Michael et al., 2014). In fact, major components of EO are known to inhibit the synthesis of vital structural and functional molecules, increase membrane permeability through their toxic effects on bacterial membranes, and disrupt proton pumps, thereby interrupting energy production (Patterson et al., 2019). These mechanisms collectively contribute to their strong antimicrobial properties, making EO potent agents against various bacterial strains.

In the present study, the strong antibacterial activity of both EO of MRM and MRT can be associated to the major chemical components identified using GC-MS/MS analysis. Indeed, rotundifolone, the major oxygenated monoterpene found in both regions (30.12 % in MRM and 24.51 % in MRT), was already described for its antimicrobial properties. In fact, Thach et al. (2013) reported that rotundifolone, the primary constituent of EO of *M. aquatica* (91.2 %), demonstrated antibacterial effects against *B. subtilis, E. coli, Pseudomonas aeruginosa, S. aureus, and Shigella flexneri,* with inhibition zones diameter ranging from 23 to 56 mm. Furthermore, other components of EO *M. rotundifolia* that contribute significantly to the antibacterial potential include chlorcarvacrol and pulegone, which were identified in notable concentrations:

chlorcarvacrol at 15.75 % in MRM and pulegone at 19.11 % in MRT. According to Shahdadi et al. (2023), these compounds well known for their antimicrobial properties may enhance the overall bioactivity of the EO. In comparison with other *Mentha* species, it has been reported that caryophyllene and (−)germacrene D, the major constituent of EO of *Mentha longifolia* (L.), demonstrated strong antimicrobial activity against *P. aeruginosa* (Tourabi et al., 2023).

3.4.2. Antifungal activity

Results of the antifungal effect of EO of MRM and MRT against the tested yeasts and molds are also presented in Table 3. As shown, both EO of MRM and MRT showed a fungicidal and/or a fungistatic effect on the tested fungal species. Unlike EO of MRM, EO of MRT showed a strong antifungal activity, achieving an inhibition zone diameter of 41.25 mm against *Rhodotorula* spp. In comparison, Amp B, used as the positive control in this study, exhibited lower inhibition zones, measuring only 12.5 mm and 13.5 mm against *C. tropicalis* and *Rhodotorula* spp., respectively. These findings are further supported by the MIC and MFC values, which confirm the higher antifungal potential of the EO when compared to Amp B. In addition, the effect of EO of *M. rotundifolia* against molds revealed remarkable effectiveness, with 100 % inhibition of EO of MRM and MRT against *A. flavus* and *A. niger* growth. This inhibition surpasses the effect of the positive control, Amp B, which exhibited only 25 % inhibition against *A. flavus* growth, and had no detectable effect on *A. niger* growth. These results are similar to those recently reported by Salamatullah (2022), who registered an antifungal activity of EO of *M. rotundifolia* sampled from the Northeast Maghreb region, achieving the largest inhibition zones diameter against *A. flavus* (51.32 ± 1.32 mm) and *A. niger* (34.51 ± 1.07 mm).

Regarding the MFC/MIC ratio, EO of MRT showed a fungicidal effect on all tested strains including *C. tropicalis, Rhodotorula* spp., *A. niger* ATCC 1015, and *A. flavus* NRRL 3357, with values ranging from 1 to 2.28. Concerning the effect of EO on the baker's yeast *S. cerevisiae,* both EO of MRM and MRT showed fungistatic effect with high MIC value of 123.07 ± 0.01 μL/mL. Although it is considered to be a non-pathogenic yeast, an increase in *S. cerevisiae* infections has recently been observed, and the species had as a wide range of resistance to chemicals, which can be a worrying problem and must therefore attract the attention of scientists to identify alternative solutions to combat emerging non-routine infections (Górzyńska et al., 2024).

Results obtained in this study highlight the strong potential of EO of *M. rotundifolia* in fighting fungal growth, similar to recent data on the antifungal effect of other aromatic and medicinal plants (Msegued Ayam et al., 2025). Comparison of the obtained results with previous studies may provide further insight into some essential characteristics of the plant investigated in this study. For example, Mimica-Dukic et al. (2003) reported an antifungal activity of EO of different *Mentha* species (*M. aquatica, M. piperita*, and *M. longifolia*) against *C. albicans*, with a MIC value of 8 μL/mL. This value is far higher that the MIC values obtained in the present study with both EO of MRM and MRT (2.13 μL/mL) against *C. tropicalis*, although comparing the antifungal activity of different EO is challenging due to the variations in EO extraction methods that could influence its chemical profile and the effectiveness of the identified bioactive components. The findings reinforce the potential of *M. rotundifolia* EO as a potent antifungal agent, offering promising prospects for broader applications .

3.5. DFT and MESP analysis

A basic method for examining the link between geometric structure and electronic characteristics of chemical compounds is Density Functional Theory (DFT) (Orio et al., 2009). This approach, based on electron density, helps to forecast interactions between molecules, atoms, or ions and offers a better knowledge of chemical reactivity (Gobi et al., 2024). Using the B3LYP approach and the 6-31G+(d,p) basis set, Gaussian 09 (Frisch et al., 2009) and GaussView 5.0 software (Dennington et al., 2009), computations were conducted in this work. Among the global electronic characteristics studied are frontier molecular orbits (HOMO and LUMO), the energy gap, and various reactivity indices: chemical potential, hardness, softness, electrophilicity, and nucleophilicity. The following equations were used to calculate these values. μ = (EHOMO + ELUMO)/2, η = EHOMO - ELUMO, S = $1/\eta$, $\omega = \mu^2/2\eta$, N = EHOMO(Nu) - EHOMO(TCE) (Salah et al., 2020; Morales-Bayuelo et al., 2020). Every optimized structure is an energy minimum (positive vibrational frequency). Total energy analysis (Fig. 2) lets one rank the stability of the compounds as follows: Chlorcarvacrol ranks higher than Rotundifolone, which ranks higher than Pulegone, which ranks higher than Piperitenone. The electrical values and reactive characteristics are also shown in Table 4 and represented in Fig. 3.

3.5.1. Frontier Molecular Orbitals (FMO)

Examining the frontier molecular orbitals HOMO and LUMO one may evaluate molecular reactivity, a fundamental concept in medicinal chemistry. The energy gap between these two orbitals reveals information on the chemical stability and reactivity of the molecules. The HOMO is linked to nucleophilic sites; the LUMO to electrophilic ones. These orbitals and the areas of electron density green: negative charges, red: positive charges are shown (Fig. 3). As shown, the stability of the compounds, depending on the values, falls in the following sequence: Chlorcarvacrol > Pulegone > Rotundifolone > Piperitenone, suggesting that chlorcarvacrol is the most reactive, yet less stable from a kinetic standpoint.

The energy values also enable the computation of several reactivity indices including chemical potential (μ), hardness, and electrophilicity. Predicting binding affinity depends mostly on the chemical potential, a fundamental sign of interactions between an active molecule and its biological target (Kaavin et al., 2024). Table 4 shows the following order of decreasing μ values: Chlorcarvacrol > Pulegone > Piperitenone > Rotundifolone, implying that Rotundifolone could have more robust interactions with biological targets. A large dipole moment value supports this affinity in line with the molecular docking findings. Examining the biological activity of compounds requires electrophilic and nucleophilic indices (Kaavin et al., 2024). While nucleophilic chemicals aim at electron-deficient areas, electrophilic ones engage with electron-rich areas. Table 4 shows that all investigated substances have significant nucleophilic character, which falls in the order: Chlorcarvacrol > Piperitenone > Pulegone > Rotundifolone (Jaramillo et al., 2008). Electrophilicity follows the opposite order: Rotundifolone > Piperitenone > Pulegone > Chlorcarvacrol, categorizing the last two as moderate electrophiles (Domingo et al., 2002). All substances seem to be suitable candidates for biological uses given these indices, together with chemical hardness and chemical potential. Pulegone and Chlorcarvacrol, on the other hand, show less activity in electron-rich and electron-deficient areas, respectively, which could account for the differences between molecular docking results and in vitro studies on bacterial and fungal strains.

3.5.2. MEP analysis

A commonly used method to find reactive sites, study charge distribution, and investigate hydrogen bonding interactions inside a molecule is Molecular Electrostatic Potential (MEP) (Lohith et al., 2022). The most electronegative areas show in red by projecting potential values onto the molecular surface, suggesting places vulnerable to electrophilic attacks; the most electropositive zones, in blue, denote nucleophilic attack sites. Intermediate areas—green, yellow, or orange show rising potentials in the sequence: red < orange < yellow < green < blue (Ali et al., 2022). The MEP maps (Fig. 4) shows that the oxygen atom of the C=O groups is a susceptible site for electrophilic assaults (red zones) in the Pulegone, Rotundifolone, and

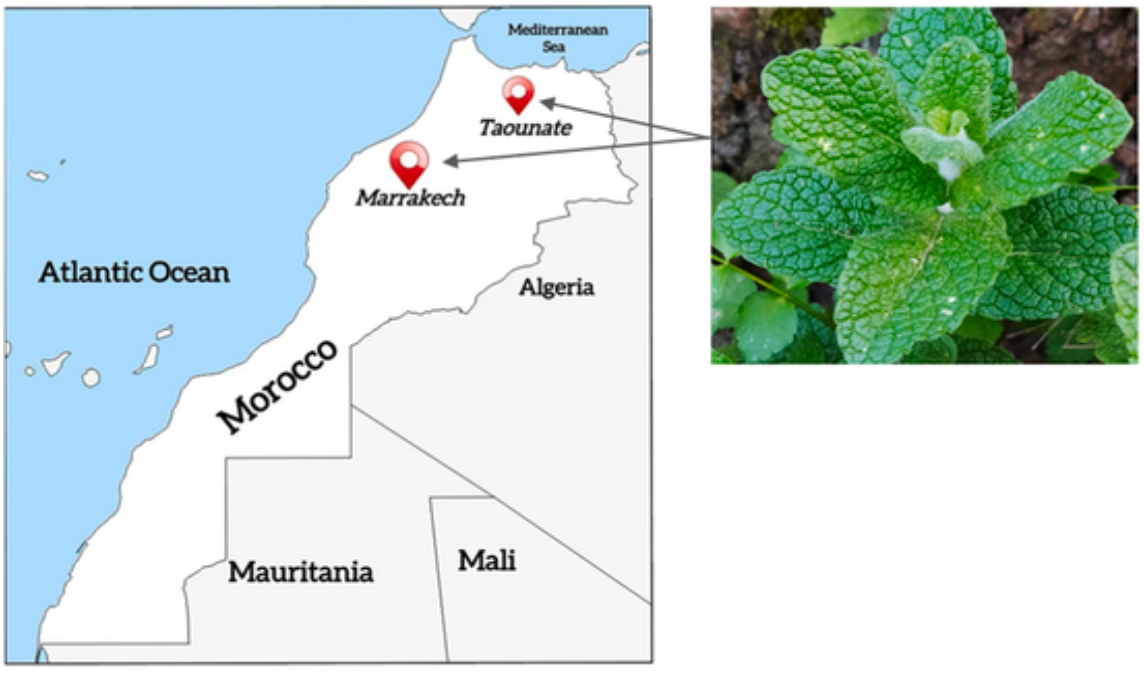

Fig. 1. Map of Morocco showing the sampling study areas of *M. rotundifolia* (*Marrakech* and *Taounate*).

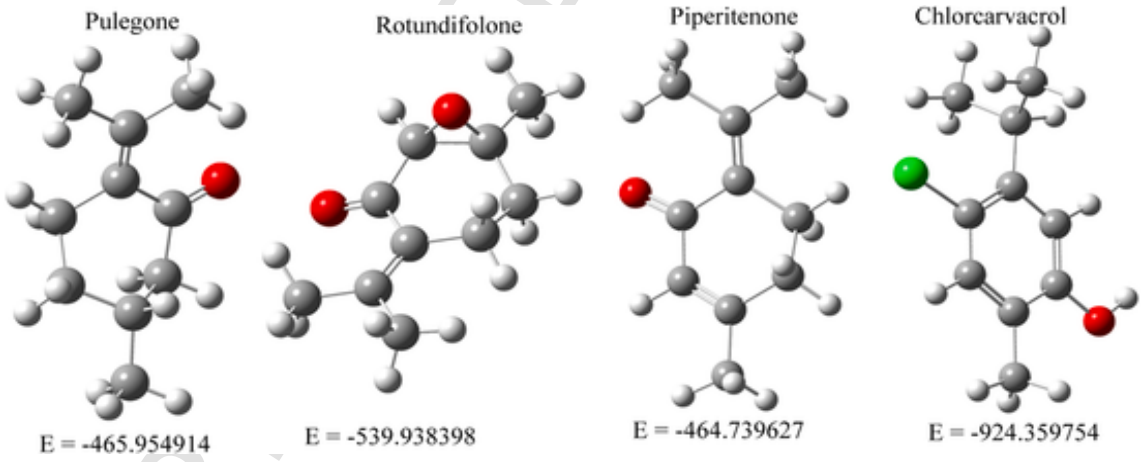

Fig. 2. Optimized structures of the compounds Pulegone, Rotundifolone, Piperitenone and Chlorcarvacrol, obtained by the DFT method at the B3LYP/6-31 + G(d,p) level, together with their energies (in eV).

Table 4
Chemical reactivity descriptors of the synthesized compounds (in eV).

Compounds	E(HOMO)	E(LUMO)	μ	X	η	ω	N	S	Md (Debye)
Chlorcarvacrol	−6.148	−0.590	−3.369	3.369	5.557	1.0214	3.260	0.179	2.346
Piperitenone	−6.493	−1.657	−4.0757	4.0757	4.835	1.717	2.915	0.206	4.151
Pulegone	−6.508	−1.401	−3.955	3.955	5.106	1.531	2.900	0.195	3.368
Rotundifolone	−6.736	−1.686	−4.211	4.211	5.0498	1.755	2.672	0.198	3.299

Note: $\mu = (E_{HOMO} + E_{LUMO})/2$; $\eta = E_{LUMO} - E_{HOMO}$; $\omega = \mu^2/2\eta$; $N = E_{HOMO(Nu)} - E_{HOMO(TCE)}$; $S = 1/\eta$, $\omega = \mu^2/(2\eta)$; $X = -\mu = -(E_{HOMO} + E_{LUMO})/2$; Md: Dipole Moment in Debye.

Piperitenone compounds. On the other hand, Chlorcarvacrol's OH alcohol group is a nucleophilic site (blue zones). MEP study also reveals that the chlorine atom (Cl) in Chlorcarvacrol sits in rather negative electrostatic potential areas (orange-yellow). These findings imply that especially via hydrogen bonds (donor or acceptor), halogen bonds, and hy-

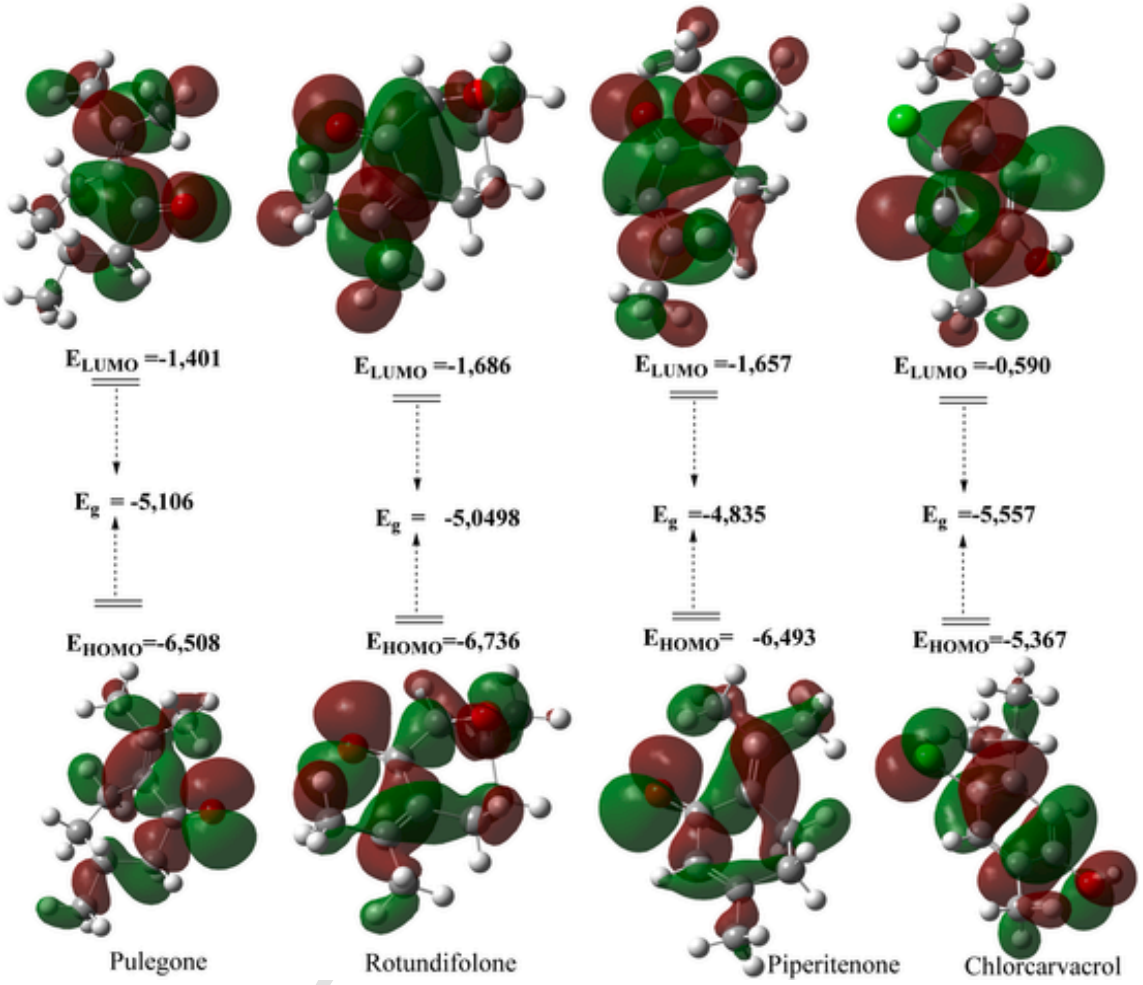

Fig. 3. EHOMO, ELUMO and Egap energy levels in (eV) for the synthesized compounds, calculated using the B3LYP/6-31G + (d,p) method.

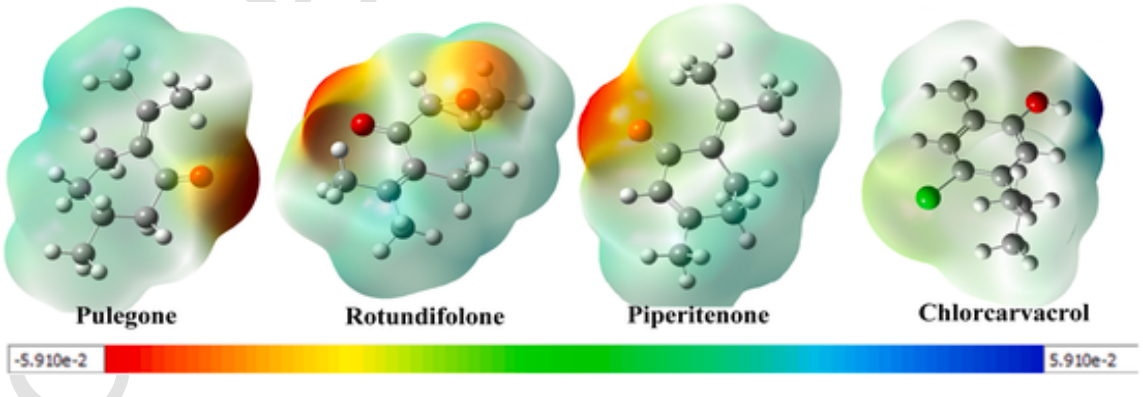

Fig. 4. MEP formed by matching the total density and the electrostatic potential in the gas phase for the compounds studied.

drophobic interactions all four chemicals can create intermolecular interactions with target protein amino acid residues.

3.6. Molecular docking

A computer method called molecular docking forecasts the interactions and preferred orientation of a tiny molecule ligand when attached to a target macromolecule, such a nucleic acid (DNA or RNA) or a protein. Playing a key role in drug discovery and design, it offers insightful analysis of binding affinity, stability, and specificity. By means of conformation space exploration and interaction energy computation, Tools like AutoDock Vina, DockThor, Glide, SwissDock, and Discovery Studio (Friesner et al., 2004; Lutsik et al., 2011; Grosdidier et al., 2011; Eberhardt et al., 2021) provide strong algorithms to simulate and assess ligan d-receptor interactions.

AutoDock Vina program and Discovery Studio software were used to investigate the molecular interactions and to maximize design strategies for analysis and visualization of docking outcomes. By lowering expenses and experimental work in the pharmaceutical and agri-food industrial research, these methods together speed the development of bioactive chemicals (drugs, additives, *etc.*), hence enabling virtual screening, hit-to-led optimization, and mechanistic knowledge.

Aiming to find possible targets among proteases from pathogenic bacteria and fungi, notably *E. coli* (PDB: 4TZK), *B. subtilis* (6UF6), and *C. tropicalis* (6T1U) were chosen from the RCSB Protein Data Bank. The choice was based on the well-documented role in key microbial processes. Regarding the first choice (PDB: 4TZK), it was supported by Khan et al. (2023) for the crucial role in protein quality control and bacterial survival under stressful conditions, making it an attractive antibacterial target. The second choice (6UF6) was considered because this protein is essential for sporulation and nutritional adaptation (Hastuti et al., 2025; Agrawal et al., 2024). The last choice (6T1U) was based also on the virulence and pathogenicity of the selected protein in fungal infections, making it a promising antifungal target (Rana et al., 2021; Zhang et al., 2022).

Molecular docking using AutoDock Vina and PyRx software evaluated the biological activity of the major compounds in the EO of MRT and MRM. Using AutoDockTools 1.5.6, the proteins were prepared by eliminating water molecules and hydrogen atoms while adding polar hydrogens and Kollman charges; the modified structures were translated into PDBQT format for docking. For each protease, a docking grid was carefully defined around the co-crystallized ligand to precisely target the active site, with grid dimensions of 36 Å × 40 Å × 36 Å centered at (−1.544, 34.716, 56.254 Å) for 4TZK (*E. coli*), 50 Å × 58 Å × 76 Å at (10.686, 13.072, 23.138 Å) for 6UF6 (*B. subtilis*), and 66 Å × 70 Å × 72 Å at (−16.857, −8.310, −35.949 Å) for 6T1U (*C. tropicalis*). From several poses produced by molecular docking for every ligand-protein complex (nine per target), the pose with the lowest binding free energy was chosen as the best configuration; then, 3D interaction analysis using Discovery Studio and 2D interaction visualization with Schrödinger's tool were performed.

3.6.1. Activity analysis of synthesized products and molecular interactions

- Activity against E. coli (study of Ligand–4TZK interactions)

Docking results showed binding affinities of −7.1 kcal/mol for chlorcarvacrol), −7.4 kcal/mol for piperitenone), −6.8 kcal/mol for pulegone, and −6.9 kcal/mol for rotundifolone (Table S1). Streptomycin displays a higher affinity of −8.2 kcal/mol, indicating that Chlorcarvacrol and Piperitenone exhibit strong inhibitory potential against *E. coli* (PDB ID = 4TZK). On the other hand, Fig. 5 illustrates the ligands positions within the 6UF6 active site and their specific molecular interactions. The key interactions for the different ligands are as follows. Chlorcarvacrol Forms Pi-Alkyl (PHE A:41, VAL A:65) and Pi-Sigma (ILE A:95) interactions. Piperitenone stabilized by a hydrogen bond (VAL A:65, 2.895 Å), Pi-Sigma (PHE A:41), and Alkyl interactions. Pulegone forms Pi-Alkyl (PHE A:41) and Alkyl interactions (ILE A:122, VAL A:65). Rotundifolone establishes hydrogen bonds (GLY A:96) and Pi-Sigma (PHE A:41) interactions.

- Activity against B. subtilis (study of Ligand–6UF6 Interactions)

The molecular docking results revealed that the synthesized ligands of chlorcarvacrol, piperitenone, pulegone, and rotundifolone demonstrate binding affinities of −6.2 kcal/mol, −6.0 kcal/mol, −5.8 kcal/mol, and −6.0 kcal/mol, respectively (Table S2). Comparatively, streptomycin, used as a standard drug, exhibits a similar binding affinity of −6.2 kcal/mol. This indicates that chlorcarvacrol, piperitenone, and rotundifolone are among the most effective inhibitors of *B. subtilis*, comparable to streptomycin (PDB ID = 6UF6). Fig. 6 illustrates the ligands positions within the 6UF6 active site and their specific molecular interactions. The key interactions for the different ligands are as follows. Chlorcarvacrol is stabilized by Pi-Sigma (PHE A:251, 3.448 Å), Pi-Alkyl (LEU A:249, TRP A:255), and Alkyl interactions. Piperitenone is stabilized by a hydrogen bond (THR A:91, 2.386 Å) and Alkyl interactions (VAL A:69, ILE A:71, ILE A:257). Pulegone is stabilized by Forms Pi-Sigma interactions (PHE A:234, 3.779 Å). Rotundifolone is stabilized by Pi-Alkyl (PHE A:251, TRP A:255) and an unfavorable acceptor-acceptor interaction (ILE A:222).

- Activity against C. tropicalis (study of Ligand–6T1U interactions)

The results of this study (Table S3) revealed that the complexes formed between proteins and the ligands chlorcarvacrol, piperitenone, pulegone, and rotundifolone exhibit binding affinities of −8.5 kcal/mol, −8.2 kcal/mol, −7.9 kcal/mol, and −7.7 kcal/mol, respectively. In comparison, amphotericin B, used as a standard antifungal compound, demonstrates a binding affinity of −9.7 kcal/mol. These findings suggest that rotundifolone and piperitenone emerge as the most effective inhibitors of *C. tropicalis*, comparable to amphotericin B (PDB ID: 6T1U). Fig. 7.1 shows the 2D visualization of interactions between the ligands (A: chlorcarvacrol, B: piperitenone, C: pulegone, D: rotundifolone, and E: amphotericin B) and the amino acids of *C. tropicalis* (PDB ID: 6T1U), highlighting the nature of these interactions. Fig. 7.2 shows also the placement of ligands within the active site of *C. tropicalis* (PDB ID: 6T1U) and the 3D visualization of interactions between the ligands (A: chlorcarvacrol, B: piperitenone, C: pulegone, D: rotundifolone, and E: amphotericin B). The docking study against *C. tropicalis* (PDB ID: 6T1U) demonstrates that the synthesized ligands of chlorcarvacrol, piperitenone, pulegone, and rotundifolone exhibited significant binding affinities, with values of −8.5 kcal/mol, −8.2 kcal/mol, −7.9 kcal/mol, and −7.7 kcal/mol, respectively. Among these, chlorcarvacrol showed the highest binding affinity, closely followed by piperitenone. However, amphotericin B, used as the standard antifungal molecule, exhibited the strongest binding affinity at −9.7 kcal/mol.

4. Conclusion

Results of this research study highlight the possible use of EO of *M. rotundifolia* as a natural antimicrobial agent against a wide range of bacterial and fungal pathogens, while also emphasizing its potential to provide alternative antioxidant substances. This increased efficacy is explained by the bioactive components identified by GC-MS/MS, particularly the major component, rotundifolone. Molecular docking simulations showed that the synthesized ligands exhibited significant inhibitory potential against *B. subtilis*, *E. coli*, and *C. tropicalis*. Among these, chlorcarvacrol and piperitenone consistently demonstrated strong binding affinities across all studies. The biological potential of EO extracted from *M. rotundifolia* leaves opens new perspectives for its use as alternative, sustainable and innovative solution for local products in the country. Moreover, further *in vivo* studies are required to validate the results for future applications.

CRediT authorship contribution statement

Meryem Benyamane: Writing – original draft, Methodology, Investigation. **Iman Msegued Ayam:** Validation, Investigation. **Soukaina Elorchi:** Software, Methodology. **Nouhaila Belasla:** Investigation. **Imane Brahimi:** Investigation. **Mohammed Salah:** Writing – review & editing, Software, Methodology. **Faouzi Errachidi:** Writing – review & editing, Methodology, Conceptualization. **Fatih Ozogul:** Writing – review & editing. **Chakib El Adlouni:** Writing – review & editing, Supervision. **Abdellah Zinedine:** Writing – review & editing, Supervision, Conceptualization.

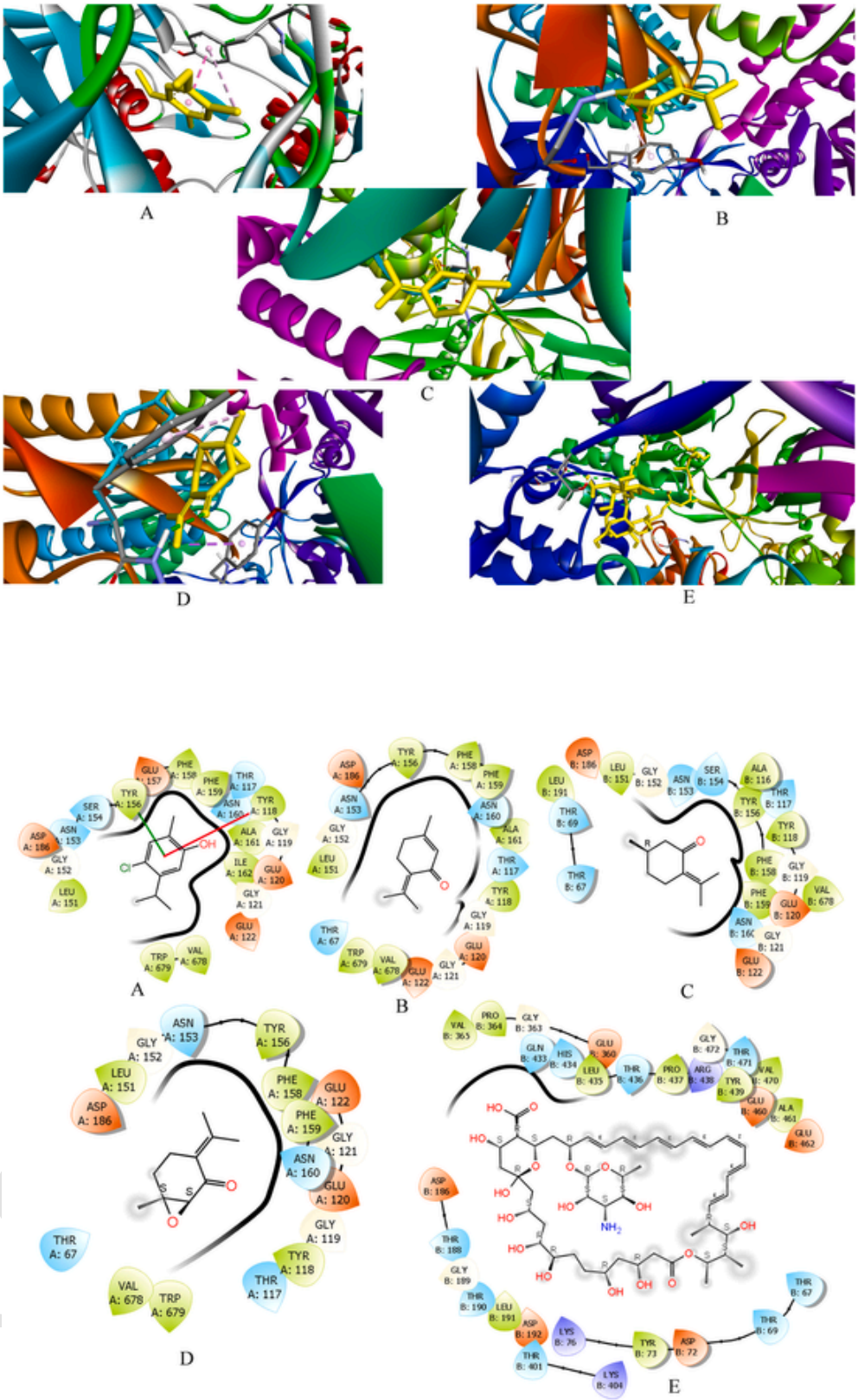

Fig. 5. (5.1): 2D visualization of interactions between the ligands; A: Chlorcarvacrol, B: Piperitenone, C: Pulegone, D: Rotundifolone, and E: Streptomycin, and the amino acids of *E. coli* (PDB ID: 4TZK), as well as the nature of these interactions. **(5.2):** Placement of ligands within the active site of *E. coli* (PDB ID: 4TZK), and A: Chlorcarvacrol, B: Piperitenone, C: Pulegone, D: Rotundifolone, and E: Streptomycin.

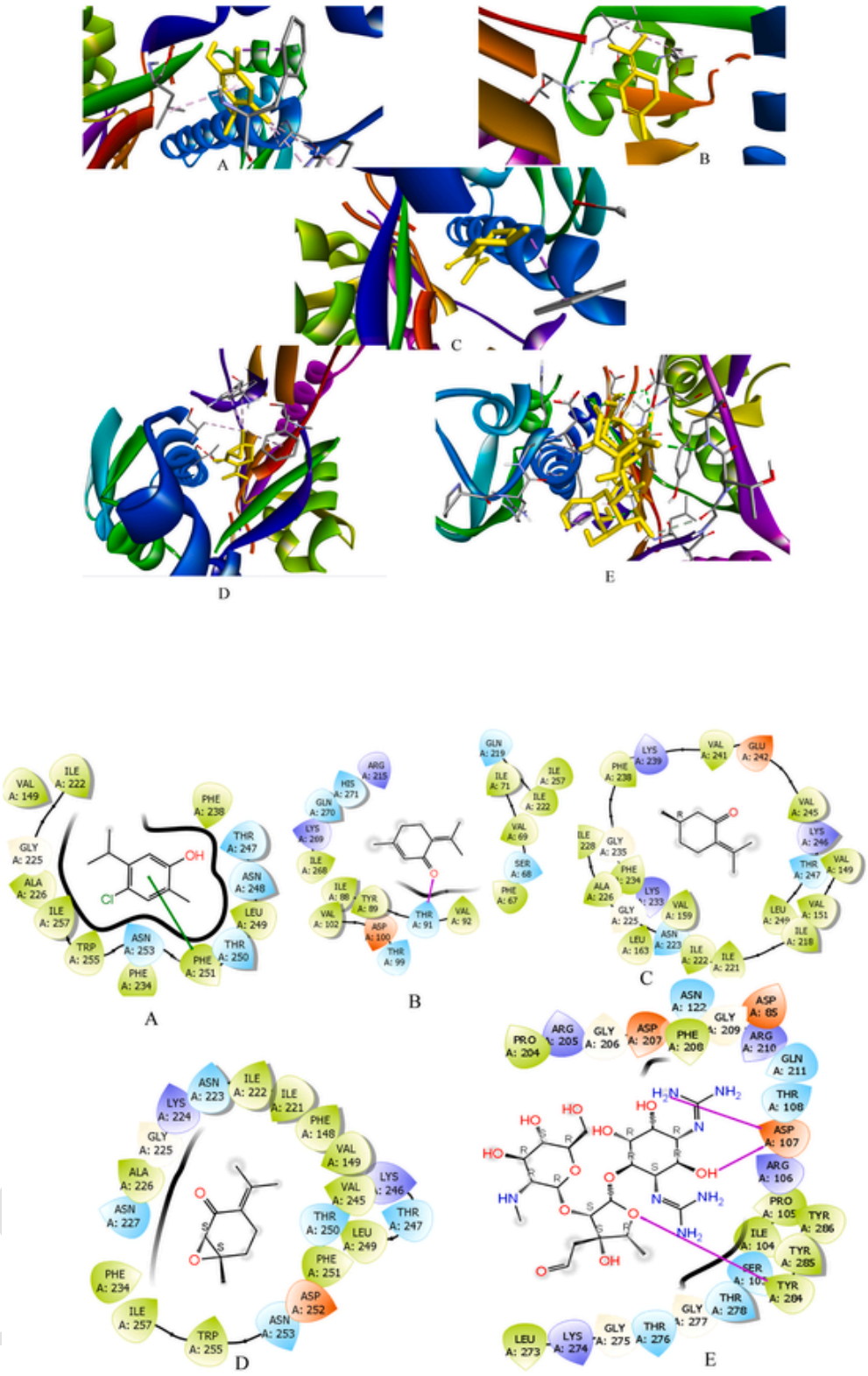

Fig. 6. (6.1): 2D visualization of interactions between the ligands; A: Chlorcarvacrol, B: Piperitenone, C: Pulegone, D: Rotundifolone, and E: Streptomycin, and the amino acids of *B. subtilis* (PDB ID: 6UF6), as well as the nature of these interactions. **(6.2)**: Placement of ligands within the active site of *B. subtilis* (PDB ID: 6UF6) and the 3D visualization of interactions between the ligands, A: Chlorcarvacrol, B: Piperitenone, C: Pulegone, D: Rotundifolone, and E: Streptomycin.

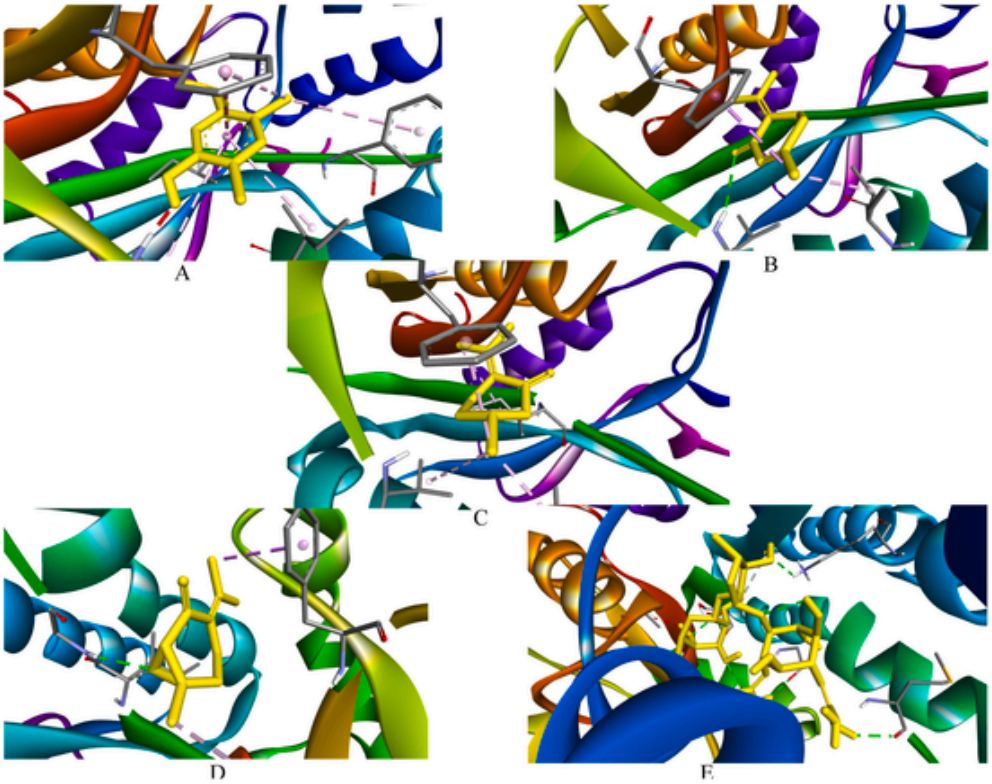
A
B
C
D
E

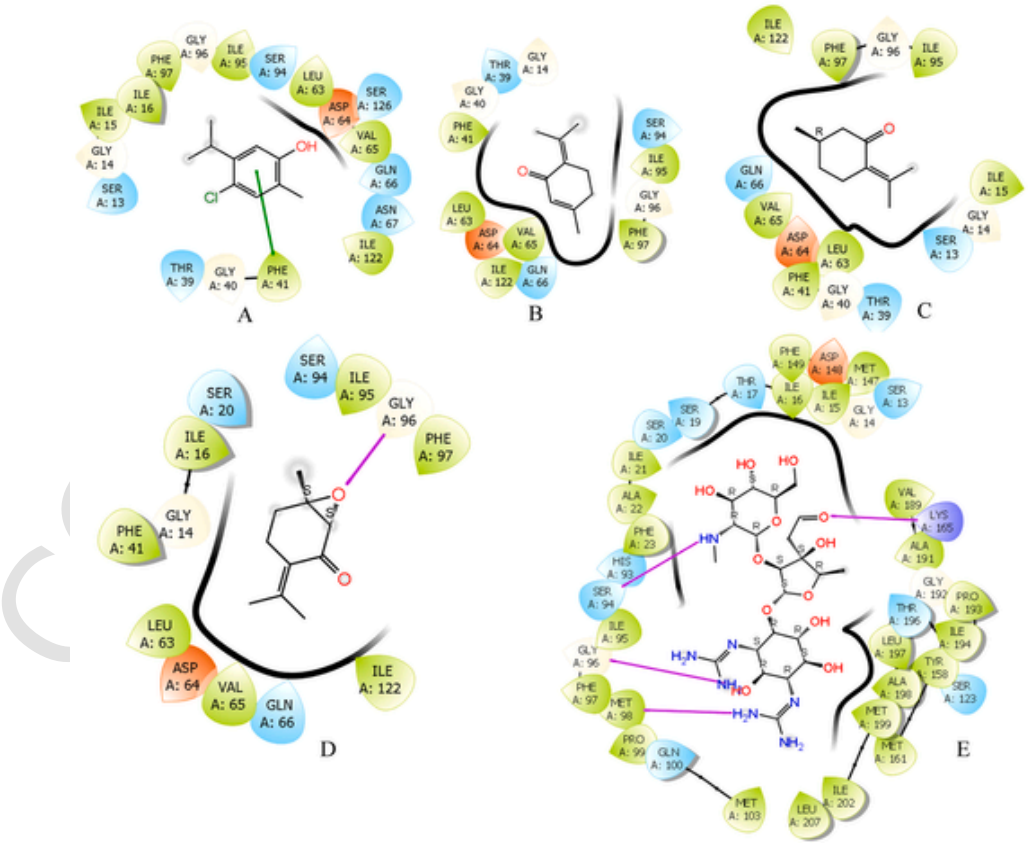
A
B
C
D
E

Fig. 7. (7.1): 2D visualization of interactions between the ligands; A: Chlorcarvacrol, B: Piperitenone, C: Pulegone, D: Rotundifolone, and E: Amphotericin B, and the amino acids of *C. tropicalis* (PDB ID: 6T1U), as well as the nature of these interactions. (7.2): Placement of ligands within the active site of *C. tropicalis* (PDB ID: 6T1U) and the 3D visualization of interactions between the ligands, A: Chlorcarvacrol, B: Piperitenone, C: Pulegone, D: Rotundifolone, and E: Amphotericin B.

Funding

This study was supported by the project "INNOSOL4MED" (PRIMA Programme supported by the European Union). A. Zinedine is most grateful to the Moroccan Ministry of Higher Education. Scientific Research and Innovation (MESRSI) and Chouaib Doukkali University (UCD) for the financial support given "**Convention (MESRSI-UCD) N°11 (2022)"**.

Declaration of competing interest

The authors declare that they have no known competing financial interests or personal relationships that could have appeared to influence the work reported in this paper.

Data availability

Data will be made available on request.

Appendix A. Supplementary data

Supplementary data to this article can be found online at https://doi.org/10.1016/j.jspr.2025.102834.

References

Agrawal, K., Patel, T.M., Thakur, S., Patel, K., Mittal, S., 2024. Quantum chemical modelling, molecular docking, synthesis and experimental anti-microbial activity of 1,4-diazepan linked piperidine derivative. Futur. J. Pharm. Sci. 10, 80. https://doi.org/10.1186/s43094-024-00652-y.

Aidi Wannes, W., Mhamdi, B., Sriti, J., Ben Jemia, M., Ouchikh, O., Hamdaoui, G., Kchouk, M.E., Marzouk, B., 2010. Antioxidant activities of the essential oils and methanol extracts from myrtle (Myrtus communis var. italica L.) leaf, stem and flower. Food Chem. Toxicol. 48, 1362–1370. https://doi.org/10.1016/j.fct.2010.03.002.

Ali, O.A.A., Elangovan, N., Mahmoud, S.F., El-Gendey, M.S., Elbasheer, H.Z.E., El-Bahy, S.M., Thomas, R., 2022. Synthesis, characterization, vibrational analysis and computational studies of a new Schiff base from pentafluoro benzaldehyde and sulfanilamide. J. Mol. Struct. 1265, 133445. https://doi.org/10.1016/j.molstruc.2022.133445.

Alonso Leite dos Santos, C., Maria Tavares Moreira, A., Rayanne da Silva Teles, B., Paul Kamdem, J., AlAsmari, A.F., Alasmari, F., Khan, M., Marivando Barros, L., Ibrahim, M., 2024. Mentha arvensis oil exhibits repellent acute toxic and antioxidant activities in Nauphoeta cinerea. Sci. Rep. 14, 1–13. https://doi.org/10.1038/s41598-024-72722-3.

Aouadi, G., Soltani, A., Grami, L.K., Abada, M. Ben, Haouel, S., Boushih, E., Chaanbi, M., Elkahoui, S., Hajlaoui, M.R., Jemâa, J.M. Ben, Taibi, F., 2021. Chemical investigations on Algerian Mentha rotundifolia and Myrtus communis essential oils and assessment of their insecticidal and antifungal activities. Int. J. Agric. Biol. 26, 666–680. https://doi.org/10.17957/IJAB/15.1881.

Ben Haj Yahia, I., Bouslimi, W., Messaoud, C., Jaouadi, R., Boussaid, M., Zaouali, Y., 2019. Comparative evaluation of Tunisian Mentha L. species essential oils: selection of potential antioxidant and antimicrobial agents. J. Essent. Oil Res. 31, 184–195. https://doi.org/10.1080/10412905.2018.1550021.

Benabdallah, A., Rahmoune, C., Boumendjel, M., Aissi, O., Messaoud, C., 2016. Total phenolic content and antioxidant activity of six wild Mentha species (Lamiaceae) from northeast of Algeria. Asian Pac. J. Trop. Biomed. 6, 760–766. https://doi.org/10.1016/j.apjtb.2016.06.016.

Brahmi, F., Hauchard, D., Guendouze, N., Madani, K., Kiendrebeogo, M., Kamagaju, L., Stévigny, C., Chibane, C., Duez, P., 2015. Phenolic composition, in vitro antioxidant effects and tyrosinase inhibitory activity of three Algerian Mentha species: M. spicata (L.), M. pulegium (L.) and M. rotundifolia (L.) Huds (Lamiaceae). Ind. Crops Prod. 74, 722–730. https://doi.org/10.1016/j.indcrop.2015.04.038.

Calo, J.R., Crandall, P.G., O'Bryan, C.A., Ricke, S.C., 2015. Essential oils as antimicrobials in food systems – a review. Food Control 54, 111–119. https://doi.org/10.1016/j.foodcont.2014.12.040.

Carneiro, A.A.J., Ferreira, I.C.F.R., Dueñas, M., Barros, L., da Silva, R., Gomes, E., Santos-Buelga, C., 2013. Chemical composition and antioxidant activity of dried powder formulations of Agaricus blazei and Lentinus edodes. Food Chem 138, 2168–2173. https://doi.org/10.1016/j.foodchem.2012.12.036.

Chauhan, A., 2014. GC-MS technique and its analytical applications in science and technology. J. Anal. Bioanal. Tech. 5. https://doi.org/10.4172/2155-9872.1000222.

Chebbac, K., Ghneim, H.K., El Moussaoui, A., Bourhia, M., El Barnossi, A., Ouaritini, Z.B., Salamatullah, A.M., Alzahrani, A., Aboul-Soud, M.A.M., Giesy, J.P., Guemmouh, R., 2022. Antioxidant and antimicrobial activities of chemically-characterized essential oil from Artemisia aragonensis lam. against drug-resistant microbes. Molecules 27. https://doi.org/10.3390/molecules27031136.

Cosentino, S., Tuberoso, C.I.G., Pisano, B., Satta, M., Mascia, V., Arzedi, E., 1999. In-vitro antimicrobial activity and chemical composition of Sardinian Thymus essential oils. 130–135. https://doi.org/10.1046/j.1472-765X.1999.00605.x.

Derwich, E., Benziane, Z., Taouil, R., Senhaji, O., Touzani, M., 2010. Comparative essential oil composition of leaves of Mentha rotundifolia and Mentha pulegium a traditional herbal medicine in Morocco. Am.-Eurasian J. Sustain. Agric. (AEJSA) 4 (1), 47–54. Available at: https://www.aensiweb.net/AENSIWEB/aejsa/aejsa/2010/47-54.pdf. (Accessed 24 September 2025).

Domingo, L.R., Aurell, M.J., Pérez, P., Contreras, R., 2002. Quantitative characterization of the global electrophilicity power of common diene/dienophile pairs in Diels-Alder reactions. Tetrahedron 58, 4417–4423. https://doi.org/10.1016/S0040-4020(02)00410-6.

Eberhardt, J., Santos-Martins, D., Tillack, A.F., Forli, S., 2021. AutoDock Vina 1.2.0: new docking methods, expanded force field, and python bindings. J. Chem. Inf. Model. 61, 3891–3898. https://doi.org/10.1021/acs.jcim.1c00203.

El Hassani, F.Z., 2020. Characterization, activities, and ethnobotanical uses of Mentha species in Morocco. Heliyon 6, e05480. https://doi.org/10.1016/j.heliyon.2020.e05480.

El Omari, N., Chamkhi, I., Balahbib, A., Benali, T., Akhazzane, M., Ullah, R., Alotaibi, A., Elouafy, Y., Elhrech, H., Bouyahya, A., 2024. GC-MS-MS analysis and biological properties determination of Mentha piperita L., essential oils. Biochem. Systemat. Ecol. 116, 104875. https://doi.org/10.1016/j.bse.2024.104875.

Friesner, R.A., Banks, J.L., Murphy, R.B., Halgren, T.A., Klicic, J.J., Mainz, D.T., Repasky, M.P., Knoll, E.H., Shelley, M., Perry, J.K., Shaw, D.E., Francis, P., Shenkin, P.S., 2004. Glide: a new approach for rapid, accurate docking and scoring. 1. Method and assessment of docking accuracy. J. Med. Chem. 47, 1739–1749. https://doi.org/10.1021/jm0306430.

Frisch, M.J., Trucks, G.W., Schlegel, H.B., Scuseria, G.E., Robb, M.A., Cheeseman, J.R., Scalmani, G., Barone, V., Mennucci, B., Petersson, G.A., Nakatsuji, H., Caricato, M., Li, X., Hratchian, H.P., Izmaylov, A.F., Bloino, J., Zheng, G., Sonnenberg, J.L., Hada, M., Ehara, M., Toyota, K., Fukuda, R., Hasegawa, J., Ishida, M., Nakajima, T., Honda, Y., Kitao, O., Nakai, H., Vreven, T., Montgomery, J.A., Peralta, J.E., Ogliaro, F., Bearpark, M., Heyd, J.J., Brothers, E., Kudin, K.N., Staroverov, V.N., Kobayashi, R., Normand, J., Raghavachari, K., Rendell, A., Burant, J.C., Iyengar, S.S., Tomasi, J., Cossi, M., Rega, N., Millam, J.M., Klene, M., Knox, J.E., Cross, J.B., Bakken, V., Adamo, C., Jaramillo, J., Gomperts, R., Stratmann, R.E., Yazyev, O., Austin, A.J., Cammi, R., Pomelli, C., Ochterski, J.W., Martin, R.L., Morokuma, K., Zakrzewski, V.G., Voth, G.A., Salvador, P., Dannenberg, J.J., Dapprich, S., Daniels, A.D., Farkas, Foresman, J.B., Ortiz, J.V., Cioslowski, J., Fox, D.J., 2009. Gaussian 09, Revision B.01. Gaussian 09, Revis. B.01, vols. 1–20. Gaussian, Inc., Wallingford CT.

Gathara, M., Kamondo, B., Mwadalu, R., Omondi, S., Kivuti, M., Wairagu, N., Oduor, T., Gachie, P., 2022. Influence of soil nutrients, tree age, and sandalwood provenances on sandalwood oil yield and quality. Int. J. For. Res. https://doi.org/10.1155/2022/1577979. . 2022.

Gobi, T., Elangovan, N., Sowrirajan, S., Islam, M.S., Sirajunnisa, A., 2024. Synthesis, characterization, DFT, vibrational analysis (FT-IR and FT-Raman), topology and molecular docking studies of 3,3′-((1E,1′E)-((sulfonylbis(4,1-phenylene)) bis (azaneylylidene)) bis (methaneylylidene)) diphenol. J. Mol. Struct. 1296, 136805. https://doi.org/10.1016/j.molstruc.2023.136805.

Górzyńska, A., Kondracka, K., Korzeniowska-Kowal, A., Nawrot, U., 2024. Antifungal susceptibility of Saccharomyces cerevisiae isolated from clinical specimens. Pathogens 13, 1–12. https://doi.org/10.3390/pathogens13030248.

Grosdidier, A., Zoete, V., Michielin, O., 2011. SwissDock, a protein-small molecule docking web service based on EADock DSS. Nucleic Acids Res. 39, 270–277. https://doi.org/10.1093/nar/gkr366.

Gulluce, M., Sahin, F., Sokmen, M., Ozer, H., Daferera, D., Sokmen, A., Polissiou, M., Adiguzel, A., Ozkan, H., 2007. Antimicrobial and antioxidant properties of the essential oils and methanol extract from Mentha longifolia L. ssp. longifolia. Food Chem. 103, 1449–1456. https://doi.org/10.1016/j.foodchem.2006.10.061.

Hastuti, L.P., Hermawan, F., Prastya, M.E., Ernawati, T., Putra, N.R., Jumina, J., Gaffar, S., Ekawardhani, S., 2025. In-silico and in-vitro study of hydroxythioxanthone derivatives as a potential candidate for antibacterial agents. Results Chem. 17, 102525. https://doi.org/10.1016/j.rechem.2025.102525.

Hazrati, S., Lotfi, K., Govahi, M., Ebadi, M.T., 2021. A comparative study: influence of various drying methods on essential oil components and biological properties of Stachys lavandulifolia. Food Sci. Nutr. 9, 2612–2619. https://doi.org/10.1002/fsn3.2218.

Jaramillo, P., Domingo, L.R., Chamorro, E., Pérez, P., 2008. A further exploration of a nucleophilicity index based on the gas-phase ionization potentials. J. Mol. Struct. THEOCHEM 865, 68–72. https://doi.org/10.1016/j.theochem.2008.06.022.

Jeldi, L., Taarabt, K.O., Mazri, M.A., Ouahmane, L., Alfeddy, M.N., 2022. Chemical composition, antifungal and antioxidant activities of wild and cultivated Origanum compactum essential oils from the municipality of Chaoun, Morocco. South Afr. J. Bot. 147, 852–858. https://doi.org/10.1016/j.sajb.2022.03.034.

Kaavin, K., Naresh, D., Yogeshkumar, M.R., Krishna Prakash, M., Janarthanan, S., Murali

Krishnan, M., Malathi, M., 2024. In-silico DFT studies and molecular docking evaluation of benzimidazo methoxy quinoline-2-one ligand and its Co, Ni, Cu and Zn complexes as potential inhibitors of Bcl-2, Caspase-3, EGFR, mTOR, and PI3K, cancer-causing proteins. Chem. Phys. Impact 8, 100418. https://doi.org/10.1016/j.chphi.2023.100418.

Khan, M.Z., Azad, A.K., Jan, S., Safdar, M., Bibi, S., Majid, A.M.S.A., Albadrani, G.M., Nouh, N.A.T., Abdulhakim, J.A., Abdel-Daim, M.M., 2023. An experimental and computational analysis of plant compounds from whole Urtica dioica L. plant's essential oil for antioxidant and antibacterial activities. Metabolites 13. https://doi.org/10.3390/metabo13040502.

Khodaei, N., Nguyen, M.M., Mdimagh, A., Bayen, S., Karboune, S., 2021. Compositional diversity and antioxidant properties of essential oils: predictive models. Lwt 138. https://doi.org/10.1016/j.lwt.2020.110684.

Khwaza, V., Aderibigbe, B.A., 2025. Antibacterial activity of selected essential oil components and their derivatives: a review. Antibiotics 14. https://doi.org/10.3390/antibiotics14010068.

Ladjel, S., Gherraf, N., Hamada, D., 2011. Antimicrobial effect of essential oils from the Algerian medicinal plant Mentha Rotundifolia L. J. Appl. Sci. Res. 7, 1665–1667.

Lecklider, T., 2011. Maintainng a heathy rhythm. EE Eval. Eng. 50, 36–39. available at: https://link.gale.com/apps/doc/A272486022/AONE?u=anon9110d3f9&sid=googleScholar&xid=284e079d. (Accessed 24 September 2025).

Li, H., Qiao, S., Zhang, S., 2025. Essential oils in grain storage: a comprehensive review of insecticidal and antimicrobial constituents, mechanisms, and applications for grain security. J. Stored Prod. Res. 111, 102537. https://doi.org/10.1016/j.jspr.2024.102537.

Lohith, T.N., Hema, M.K., Karthik, C.S., Sandeep, S., Mallesha, L., Mallu, P., Jothi Ramalingam, R., Sridhar, M.A., Karnan, M., Lokanath, N.K., 2022. N-[2-(5-bromo-2-chloro-pyrimidin-4-yl)thio)-4-methoxy-phenyl]-4-chlorobenzenesulfonamide: the existence of H-bond and halogen bond interactions assisted supramolecular architecture – a quantum chemical investigation. J. Mol. Struct. 1267, 133476. https://doi.org/10.1016/j.molstruc.2022.133476.

Lutsik, P., Feuerbach, L., Arand, J., Lengauer, T., Walter, J., Bock, C., 2011. BiQ Analyzer HT: Locus-specific analysis of DNA methylation by high-throughput bisulfite sequencing. Nucleic Acids Res. 39, 551–556. https://doi.org/10.1093/nar/gkr312.

Maškovič, P.Z., Manojlovič, N.T., Mandič, A.I., Mišan, A.Ç., Milovanovic, I.L., Radojkovič, M.M., Cvijovič, M.S., Solujič, S.R., 2012. Fitohemija i biološka aktivnost ekstrakata biljne vrste Halacsya sendtneri (Boiss.) Dörfl. Hem. Ind. 66, 43–51. https://doi.org/10.2298/HEMIND110828068M.

Meenu, M., Padhan, B., Patel, M., Patel, R., Xu, B., 2023. Antibacterial activity of essential oils from different parts of plants against Salmonella and Listeria spp. Food Chem. 404, 134723. https://doi.org/10.1016/j.foodchem.2022.134723.

Messaoudi, M., Rebiai, A., Sawicka, B., Atanassova, M., Ouakouak, H., Larkem, I., Egbuna, C., Awuchi, C.G., Boubekeur, S., Ferhat, M.A., Begaa, S., Benchikha, N., 2022. Effect of extraction methods on polyphenols, flavonoids, mineral elements, and biological activities of essential oil and extracts of *Mentha pulegium*. Molecules 27. https://doi.org/10.3390/molecules27010011.

Michael, C.A., Dominey-Howes, D., Labbate, M., 2014. The antimicrobial resistance crisis: causes, consequences, and management. Front. Public Health 2, 1–8. https://doi.org/10.3389/fpubh.2014.00145.

Mimica-Dukic, N., Bozin, B., Sokovic, M., Mihajlovic, B., Matavulj, M., 2003. Antimicrobial and antioxidant activities of essential oils of. Planta Med. 69, 413–419. https://doi.org/10.1055/s-2003-39704.

Miraliakbari, H., Shahidi, F., 2008. Antioxidant activity of minor components of tree nut oils. Food Chem. 111, 421–427. https://doi.org/10.1016/j.foodchem.2008.04.008.

Moattar, F.S., Sariri, R., Yaghmaee, P., Giahi, M., 2016. Enzymatic and non-enzymatic antioxidants of Calamintha officinalis moench extracts. J. Appl. Biotechnol. Rep. 3, 489–494. Available at: https://www.biotechrep.ir/article_69239_43d3ef649b9660e9393b708a98acfd07.pdf. (Accessed 24 September 2025).

Morales-Bayuelo, A., Sánchez-Márquez, J., Jana, G., Chattaraj, P.K., 2020. A conceptual DFT analysis of the plausible mechanism of some pericyclic reactions. Struct. Chem. 31, 1745–1756. https://doi.org/10.1007/s11224-020-01527-7.

Msegued Ayam, I., Zinedine, A., Lyagoubi, A., Rocha, J.M., Raoui, S.M., Errachidi, F., 2025. Chemical composition, antioxidant, and antifungal activity of essential oil extracted from cumin seeds (Cuminum cyminum L.) planted in Morocco. Chem. Biodivers. 22. https://doi.org/10.1002/cbdv.202402687.

Mwithiga, G., Maina, S., Gitari, J., Muturi, P., 2022. Rosemary (Rosmarinus officinalis L.) growth rate, oil yield and oil quality under differing soil amendments. Heliyon 8, e09277. https://doi.org/10.1016/j.heliyon.2022.e09277.

Nickavar, B., Alinaghi, A., Kamalinejad, M., 2008. Evaluation of the antioxidant properties of five Mentha species. Iran. J. Pharm. Res. (IJPR) 7, 203–209. Available at: https://brieflands.com/articles/ijpr-128592.pdf. (Accessed 24 September 2025).

Noshad, M., Alizadeh Behbahani, B., Nikfarjam, Z., 2022. Chemical composition, antibacterial activity and antioxidant activity of Citrus bergamia essential oil: molecular docking simulations. Food Biosci. 50, 102123. https://doi.org/10.1016/j.fbio.2022.102123.

Orio, M., Pantazis, D.A., Neese, F., 2009. Density functional theory. Photosynth. Res. 102, 443–453. https://doi.org/10.1007/s11120-009-9404-8.

Patterson, J.E., McElmeel, L., Wiederhold, N.P., 2019. In vitro activity of essential oils against gram-positive and gram-negative clinical isolates, including carbapenem-resistant enterobacteriaceae. Open Forum Infect. Dis. 6, 1–4. https://doi.org/10.1093/ofid/ofz502.

Puvača, N., Milenković, J., Galonja Coghill, T., Bursić, V., Petrović, A., Tanasković, S., Pelić, M., Ljubojević Pelić, D., Miljković, T., 2021. Antimicrobial activity of selected essential oils against selected pathogenic bacteria: in vitro study. Antibiotics 10. https://doi.org/10.3390/antibiotics10050546.

Rana, L., Rai, A., Tewari, L.M., Chopra, N., Pandey, N.C., Tewari, G., 2021. Drying potential of leaves oil of DC from North India. Open Bioact. Compd. J. 9, 9–14. https://doi.org/10.2174/1874847302109010009.

Reis, F.S., Martins, A., Barros, L., Ferreira, I.C.F.R., 2012. Antioxidant properties and phenolic profile of the most widely appreciated cultivated mushrooms: a comparative study between in vivo and in vitro samples. Food Chem. Toxicol. 50, 1201–1207. https://doi.org/10.1016/j.fct.2012.02.013.

Riahi, L., Elferchichi, M., Ghazghazi, H., Jebali, J., Ziadi, S., Aouadhi, C., Chograni, H., Zaouali, Y., Zoghlami, N., Mliki, A., 2013. Phytochemistry, antioxidant and antimicrobial activities of the essential oils of Mentha rotundifolia L. in Tunisia. Ind. Crops Prod. 49, 883–889. https://doi.org/10.1016/j.indcrop.2013.06.032.

Riaz, U., Iqbal, S., Sohail, M.I., Samreen, T., Ashraf, M., Akmal, F., Siddiqui, A., Ahmad, I., Naveed, M., Khan, N.I., Akhter, R.M., 2021. A comprehensive review on emerging importance and economical potential of medicinal and aromatic plants (MAPs) in Current scenario. Pakistan J. Agric. Res. 34, 381–392. https://doi.org/10.17582/journal.pjar/2021/34.2.381.392.

Saba, I., Anwar, F., Ahmad, N., Iqbal, M., Abbas, A., Iqbal, S., Nazir, A., Al-Mijalli, S.H., 2024. Spearmint (Mentha spicata L.) leaves essential oil: comparative compositional and biological attributes as a function of different agroclimatic regions. Biocatal. Agric. Biotechnol. 56, 102984. https://doi.org/10.1016/j.bcab.2023.102984.

Sah, G., Mahawer, S.K., Bhatt, P., Shah, G.C., Kumar, R., Kumar, S., Pathak, M., Sah, A.N., 2024. Comprehensive analysis of Mentha longifolia subsp. himalaiensis essential oil: GC MS profiling and biological properties. J. Indian Chem. Soc. 101, 101160. https://doi.org/10.1016/j.jics.2024.101160.

Salah, M., Zeroual, A., Jorio, S., El hadki, H., Kabbaj, O.K., Marakchi, K., Komiha, N., 2020. Theoretical study of the 1,3-DC reaction between fluorinated alkynes and azides: reactivity indices, transition structures, IGM and ELF analysis. J. Mol. Graph. Model. 94, 107458. https://doi.org/10.1016/j.jmgm.2019.107458.

Salamatullah, A.M., 2022. Identification of volatile compounds and antioxidant, antibacterial, and antifungal properties against drug-resistant microbes of essential oils from the leaves of Mentha rotundifolia var. apodysa Briq. (Lamiaceae). Open Chem. 20, 484–493. https://doi.org/10.1515/chem-2022-0161.

Sbai, A., Talbi, F.Z., El Omari, H., Chaouche, A., Moussa, O., El Kabous, K., Barrahi, M., El-Akhal, F., Alaoui, M.M., El Khayyat, F., Ouhssine, M., 2023. Inhibitory effect of essential oil from rond left mint (Mentha Rotundifolia) on the corrosion of C35 mild steel in an acidic environment. Trop. J. Nat. Prod. Res. 7, 5628–5632. https://doi.org/10.26538/tjnpr/v7i12.38.

Shahdadi, F., Faryabi, M., Khan, H., Sardoei, A.S., Fazeli-Nasab, B., Goh, B.H., Goh, K.W., Tan, C.S., 2023. Mentha longifolia essential oil and pulegone in edible coatings of alginate and chitosan: effects on pathogenic bacteria in lactic cheese. Molecules 28. https://doi.org/10.3390/molecules28114554.

Tafrihi, M., Imran, M., Tufail, T., Gondal, T.A., Caruso, G., Sharma, S., Sharma, R., Atanassova, M., Atanassov, L., Fokou, P.V.T., Pezzani, R., 2021. The wonderful activities of the genus Mentha: not only antioxidant properties. Molecules 26, 1–22. https://doi.org/10.3390/molecules26041118.

Talbaoui, A., 2012. Chemical composition and antibacterial activity of essential oils from six Moroccan plants. J. Med. Plants Res. 6, 4593–4600. https://doi.org/10.5897/jmpr10.078.

Tewari, H., Kasana, V.K., Jyothi, K.N., Tewari, G., 2024. Efficacy of essential oils from three Mentha species against postharvest groundnut pest, Caryedon serratus (Olivier) (Coleoptera: bruchidae). J. Nat. Pestic. Res. 7, 100063. https://doi.org/10.1016/j.napere.2023.100063.

Thach, L.N., Nhung, T.H., My, V.T.N., Tran, H.A., 2013. The new rich source of rotundifolone: Mentha aquatica Linn. var. crispa oil from microwave-assisted hydrodistillation. J. Essent. Oil Res. 25, 39–43. https://doi.org/10.1080/10412905.2013.759360.

Thakker, M.R., Parikh, J.K., Desai, M.A., 2016. Isolation of essential oil from the leaves of Cymbopogon martinii using hydrodistillation : effect on yield of essential oil , yield of geraniol and antimicrobial activity 5026. https://doi.org/10.1080/0972060X.2016.1231087.

Tourabi, M., Nouioura, G., Touijer, H., Baghouz, A., El Ghouizi, A., Chebaibi, M., Bakour, M., Ousaaid, D., Almaary, K.S., Nafidi, H.-A., Bourhia, M., Farid, K., Lyoussi, B., Derwich, E., 2023. Antioxidant, antimicrobial, and insecticidal properties of chemically characterized essential oils extracted from Mentha longifolia: in vitro and in silico analysis. Plants 12, 3783. https://doi.org/10.3390/plants12213783.

Trott, O., Olson, A.J., 2010. AutoDock vina: improving the speed and accuracy of docking with a new scoring function, efficient optimization, and multithreading. J. Comput. Chem. 31, 455–461. https://doi.org/10.1002/jcc.21334.

Tumen, I., Hafizoglu, H., Kilic, A., Dönmez, I.E., Sivrikaya, H., Reunanen, M., 2010. Yields and constituents of essential oil from cones of Pinaceae spp. natively grown in Turkey. Molecules 15, 5797–5806. https://doi.org/10.3390/molecules15085797.

Wahba, H.E., Rabbu, H.S.A., Ibrahim, M.E., 2020. Evaluation of essential oil isolated from dry coriander seeds and recycling of the plant waste under different storage conditions. Bull. Natl. Res. Cent. https://doi.org/10.1186/s42269-020-00448-z.

Yakhlef, G., Hambaba, L., Pinto, D.C.G.A., Silva, A.M.S., 2020. Chemical composition and insecticidal, repellent and antifungal activities of essential oil of Mentha rotundifolia (L.) from Algeria. Ind. Crops Prod. 158, 112988. https://doi.org/10.1016/j.indcrop.2020.112988.

Yakoubi, R., Benouchenne, D., Bendjedid, S., Megateli, S., Sadok, T.H., Gali, L., Azri, O., 2024. Chemical constituents and in vitro biological activities of Mentha rotundifolia's essential oils extracted by ultrasound-assisted hydrodistillation compared to conventional hydrodistillation. Biomass Convers. Biorefinery. https://doi.org/10.1007/s13399-024-05336-4.

Yeddes, W., Gadhoumi, H., Affes, T.G., Majdi, H., 2022. Effects of grinding and bioclimatic variation on the quality and composition of the Tunisia rosemary essential oils. J. New Sci. 88, 4954–4960. https://doi.org/10.55416/sunb.jns01.2204.08801.

Yousefian, S., Esmaeili, F., Lohrasebi, T., 2023. A comprehensive review of the key

characteristics of the genus Mentha, natural compounds and biotechnological approaches for the production of secondary metabolites. Iran. J. Biotechnol. 21, 2–29. https://doi.org/10.30498/ijb.2023.380485.3605.

Zhang, P., Tangadanchu, V.K.R., Zhou, C., 2022. Identification of novel antifungal skeleton of hydroxyethyl naphthalimides with synergistic potential for chemical and dynamic treatments. Molecules 27. https://doi.org/10.3390/molecules27238453.

Zhao, D., Xu, Y.W., Yang, G.L., Husaini, A.M., Wu, W., 2013. Variation of essential oil of Mentha haplocalyx Briq. and Mentha spicata L. from China. Ind. Crops Prod. 42, 251–260. https://doi.org/10.1016/j.indcrop.2012.06.010.